El-Neaj et al. *EPJ Quantum Technology* (2020) 7:6
https://doi.org/10.1140/epjqt/s40507-020-0080-0

EPJ Quantum Technology
a SpringerOpen Journal

EPJ.org

RESEARCH Open Access

AEDGE: Atomic Experiment for Dark Matter and Gravity Exploration in Space

Yousef Abou El-Neaj[1], Cristiano Alpigiani[2], Sana Amairi-Pyka[3], Henrique Araújo[4], Antun Balaž[5], Angelo Bassi[6], Lars Bathe-Peters[7], Baptiste Battelier[8], Aleksandar Belić[5], Elliot Bentine[9], José Bernabeu[10], Andrea Bertoldi[8†], Robert Bingham[11,12], Diego Blas[13], Vasiliki Bolpasi[14], Kai Bongs[15†], Sougato Bose[16], Philippe Bouyer[8†], Themis Bowcock[17], William Bowden[18], Oliver Buchmueller[4*†], Clare Burrage[19], Xavier Calmet[20], Benjamin Canuel[8†], Laurentiu-Ioan Caramete[21†], Andrew Carroll[17], Giancarlo Cella[22], Vassilis Charmandaris[23], Swapan Chattopadhyay[24,25], Xuzong Chen[26], Maria Luisa Chiofalo[27,28], Jonathon Coleman[17†], Joseph Cotter[4], Yanou Cui[29], Andrei Derevianko[30], Albert De Roeck[31,32†], Goran S. Djordjevic[33], Peter Dornan[4], Michael Doser[32], Ioannis Drougkakis[14], Jacob Dunningham[20], Ioana Dutan[21], Sajan Easo[34], Gedminas Elertas[17], John Ellis[13,35,36†], Mai El Sawy[37,38], Farida Fassi[39], Daniel Felea[21], Chen-Hao Feng[8], Robert Flack[16], Chris Foot[9], Ivette Fuentes[40], Naceur Gaaloul[41], Alexandre Gauguet[42], Remi Geiger[43], Valerie Gibson[44], Gian Giudice[36], Jon Goldwin[15], Oleg Grachov[45], Peter W. Graham[46†], Dario Grasso[27,28], Maurits van der Grinten[34], Mustafa Gündogan[3], Martin G. Haehnelt[47†], Tiffany Harte[44], Aurélien Hees[43†], Richard Hobson[18], Jason Hogan[46†], Bodil Holst[48], Michael Holynski[15], Mark Kasevich[46], Bradley J. Kavanagh[49], Wolf von Klitzing[14†], Tim Kovachy[50], Benjamin Krikler[51], Markus Krutzik[3†], Marek Lewicki[13,52†], Yu-Hung Lien[16], Miaoyuan Liu[26], Giuseppe Gaetano Luciano[53], Alain Magnon[54], Mohammed Attia Mahmoud[55], Sarah Malik[4], Christopher McCabe[13†], Jeremiah Mitchell[24], Julia Pahl[3], Debapriya Pal[14], Saurabh Pandey[14], Dimitris Papazoglou[56], Mauro Paternostro[57], Bjoern Penning[58], Achim Peters[3†], Marco Prevedelli[59], Vishnupriya Puthiya-Veettil[60], John Quenby[4], Ernst Rasel[41†], Sean Ravenhall[9], Jack Ringwood[17], Albert Roura[61†], Dylan Sabulsky[8†], Muhammed Sameed[62], Ben Sauer[4], Stefan Alaric Schäffer[63], Stephan Schiller[64†], Vladimir Schkolnik[3], Dennis Schlippert[41], Christian Schubert[41†], Haifa Rejeb Sfar[31], Armin Shayeghi[65], Ian Shipsey[9], Carla Signorini[27,28], Yeshpal Singh[15†], Marcelle Soares-Santos[58], Fiodor Sorrentino[66†], Timothy Sumner[4], Konstantinos Tassis[14], Silvia Tentindo[67], Guglielmo Maria Tino[68,69†], Jonathan N. Tinsley[68], James Unwin[70], Tristan Valenzuela[71], Georgios Vasilakis[14], Ville Vaskonen[13,35†], Christian Vogt[72], Alex Webber-Date[17], André Wenzlawski[73], Patrick Windpassinger[73], Marian Woltmann[72], Efe Yazgan[74], Ming-Sheng Zhan[75†], Xinhao Zou[8] and Jure Zupan[76]

*Correspondence:
o.buchmueller@imperial.ac.uk
[4]Blackett Laboratory, Imperial College London, London, UK
Full list of author information is available at the end of the article
†The White Paper authors are listed with a dagger sign.

© The Author(s) 2020. This article is licensed under a Creative Commons Attribution 4.0 International License, which permits use, sharing, adaptation, distribution and reproduction in any medium or format, as long as you give appropriate credit to the original author(s) and the source, provide a link to the Creative Commons licence, and indicate if changes were made. The images or other third party material in this article are included in the article's Creative Commons licence, unless indicated otherwise in a credit line to the material. If material is not included in the article's Creative Commons licence and your intended use is not permitted by statutory regulation or exceeds the permitted use, you will need to obtain permission directly from the copyright holder. To view a copy of this licence, visit http://creativecommons.org/licenses/by/4.0/.

Springer

Abstract

We propose in this White Paper a concept for a space experiment using cold atoms to search for ultra-light dark matter, and to detect gravitational waves in the frequency range between the most sensitive ranges of LISA and the terrestrial LIGO/Virgo/KAGRA/INDIGO experiments. This interdisciplinary experiment, called Atomic Experiment for Dark Matter and Gravity Exploration (AEDGE), will also complement other planned searches for dark matter, and exploit synergies with other gravitational wave detectors. We give examples of the extended range of sensitivity to ultra-light dark matter offered by AEDGE, and how its gravitational-wave measurements could explore the assembly of super-massive black holes, first-order phase transitions in the early universe and cosmic strings. AEDGE will be based upon technologies now being developed for terrestrial experiments using cold atoms, and will benefit from the space experience obtained with, e.g., LISA and cold atom experiments in microgravity.

KCL-PH-TH/2019-65, CERN-TH-2019-126

1 Preface

This article originates from the *Workshop on Atomic Experiments for Dark Matter and Gravity Exploration* [1], which took place on July 22 and 23, 2019, hosted by CERN, Geneva, Switzerland.

This workshop reviewed the landscape of cold atom technologies being developed to explore fundamental physics, astrophysics and cosmology—notably ultra-light dark matter and gravitational effects, particularly gravitational waves in the mid-frequency band between the maximal sensitivities of existing and planned terrestrial and space experiments, and searches for new fundamental interactions—which offer several opportunities for ground-breaking discoveries.

The goal of the workshop was to bring representatives of the cold atom community together with colleagues from the particle physics and gravitational communities, with the aim of preparing for ESA the White Paper that is the basis for this article. It outlines in Sects. 2 and 3 the science case for a future space-based cold atom detector mission discussed in Sect. 4, based on technologies described in Sect. 5, and is summarized in Sect. 6.

2 Science case

Two of the most important issues in fundamental physics, astrophysics and cosmology are the nature of dark matter (DM) and the exploration of the gravitational wave (GW) spectrum.

Multiple observations from the dynamics of galaxies and clusters to the spectrum of the cosmological microwave background (CMB) radiation measured by ESA's Planck satellite and other [2] experiments indicate that there is far more DM than conventional matter in the Universe, but its physical composition remains a complete mystery. The two most popular classes of DM scenario invoke either coherent waves of ultra-light bosonic fields, or weakly-interacting massive particles (WIMPs). In the absence so far of any positive indications for WIMPs from accelerator and other laboratory experiments, there is increasing interest in ultra-light bosonic candidates, many of which appear in theories that address other problems in fundamental physics. *Such bosons are among the priority targets for AEDGE.*

The discovery of GWs by the LIGO [3] and Virgo [4] laser interferometer experiments has opened a new window on the Universe, through which waves over a wide range of frequencies can provide new information about high-energy astrophysics and cosmology. Just as astronomical observations at different wavelengths provide complementary information about electromagnetic sources, measurements of GWs in different frequency bands are complementary and synergistic. In addition to the ongoing LIGO and Virgo experiments at relatively high frequencies $\gtrsim$10 Hz, which will soon be joined by the KAGRA [5] detector in Japan and the INDIGO project [6] to build a LIGO detector in India, with the Einstein Telescope (ET) [7, 8] and Cosmic Explorer (CE) [9] experiments being planned for similar frequency ranges, ESA has approved for launch before the period being considered for Voyage 2050 missions the LISA mission, which will be most sensitive at frequencies $\lesssim 10^{-1}$ Hz, and the Taiji [10] and TianQin [11] missions proposed in China will have similar sensitivity to LISA. AEDGE is optimized for the mid-frequency range between LISA/Taiji/TianQin and LIGO/Virgo/KAGRA/INDIGO/ET/CE.[a] This range is ideal for probing the formation of the super-massive black holes known to be present in many galaxies. Also, AEDGE's observations of astrophysical sources will complement those by other GW experiments at lower and higher frequencies, completing sets of measurements from inspiral to merger and ringdown, yielding important synergies as we illustrate below. *GWs are the other priority targets for AEDGE.*

In addition to these primary scientific objectives, several other potential objectives for cold atom experiments in space are under study. These may include searches for astrophysical neutrinos, constraining possible variations in fundamental constants, probing dark energy, and probing basic physical principles such as Lorentz invariance and quantum mechanics. Cold quantum gases provide powerful technologies that are already mature for the AEDGE goals, while also developing rapidly [12]. The developments of these technologies can be expected to offer AEDGE more possibilities on the Voyage 2050 time scale. *AEDGE is a uniquely interdiscplinary and versatile mission.*

An atom interferometer such as AEDGE is sensitive to fluctuations in the relative phase between cold atom clouds separated by a distance L:

$$\Delta\phi = \omega_A \times (2L), \tag{2.1}$$

where ω_A is the frequency of the atomic transition being studied. DM interactions with the cold atoms could induce variations $\delta\omega_A$ in this frequency, and the passage of a GW inducing a strain h would induce a phase shift via a change $\delta L = hL$ in the distance of separation. The AEDGE capabilities for DM detection are summarized in Sect. 3.1, where we show how AEDGE can explore the parameters of ultra-light DM models orders of magnitude beyond current bounds. The AEDGE capabilities for GW measurements are discussed in Sect. 3.2, where we stress its unique capabilities for detecting GWs from the mergers of intermediate-mass black holes, as well as from first-order phase transitions in the early universe and cosmic strings. Finally, AEDGE prospects for other fundamental physics topics are outlined in Sect. 3.3. One specific measurement concept is described in Sect. 4, but other concepts can be considered, as reviewed in Sect. 5. The cold atom projects mentioned there may be considered as "pathfinders" for the AEDGE mission, providing a roadmap towards its realization that is outlined in Sect. 6. These experiments include many terrestrial cold atom experiments now being prepared or proposed, space

experiments such as cold atom experiments on the ISS, LISA Pathfinder and LISA itself. With this roadmap in mind, the AEDGE concept is being proposed by experts in the cold atom community, as well as GW experts and fundamental particle physicists.

3 AEDGE capabilities for its scientific priorities

In this section we develop the science case of AEDGE, providing important examples of its capabilities for its primary scientific objectives, namely the DM search and GW detection, and mentioning also other potential science topics. The basis of the sensitivity projections shown here is defined in Sect. 4.

3.1 Dark matter

Multiple observations point to the existence of dark matter (DM), an elusive form of matter that comprises around 84% of the matter energy density in the Universe [2]. So far, all of the evidence for DM arises through its gravitational interaction, which provides little insight into the DM mass, but it is anticipated that DM also interacts with normal matter through interactions other than gravity.

The direct search for DM, which aims to detect the non-gravitational interaction of DM in the vicinity of the Earth, is one of the most compelling challenges in particle physics. The direct search for DM in the form of an (electro-)weakly-interacting massive particle (WIMP) with a mass in the GeV to multi-TeV window is mature, and experiments now probe interaction cross-sections far below the electroweak scale. As yet, no positive detections have been reported (see e.g., the constraints from XENON1T [13]), and the same is true of collider searches for WIMPs and indirect searches among cosmic rays and γ rays for the products of annihilations of astrophysical WIMPs. Although the experimental search for electroweak-scale DM has been the most prominent, theoretical extensions of the Standard Model (SM) of particle physics provide many other elementary particle candidates for DM over a much wider mass scale: ranging from 10^{-22} eV to the Planck scale $\sim 10^{18}$ GeV [14].

Ultra-light DM (with a sub-eV mass) is particularly interesting, as there are many well-motivated candidates. These include the QCD axion and axion-like-particles (ALPs); (dark) vector bosons; and light scalar particles such as moduli, dilatons or the relaxion. Ultra-light bosons are also good DM candidates: there are well-understood mechanisms to produce the observed abundance (e.g., the misalignment mechanism [15–17]), and the DM is naturally cold, so it is consistent with the established structure formation paradigm.

3.1.1 Scalar dark matter

Atom interferometers are able to measure a distinctive signature of scalar DM [18, 19]. Scalar DM may cause fundamental parameters such as the electron mass and electromagnetic fine-structure constant to oscillate in time, with a frequency set by the mass of the scalar DM and an amplitude determined by the DM mass and local DM density [20, 21]. This in turn leads to a temporal variation of atomic transition frequencies, since the transition frequencies depend on the electron mass and fine-structure constant. A non-trivial signal phase occurs in a differential atom interferometer when the period of the DM wave matches the total duration of the interferometric sequence [19].

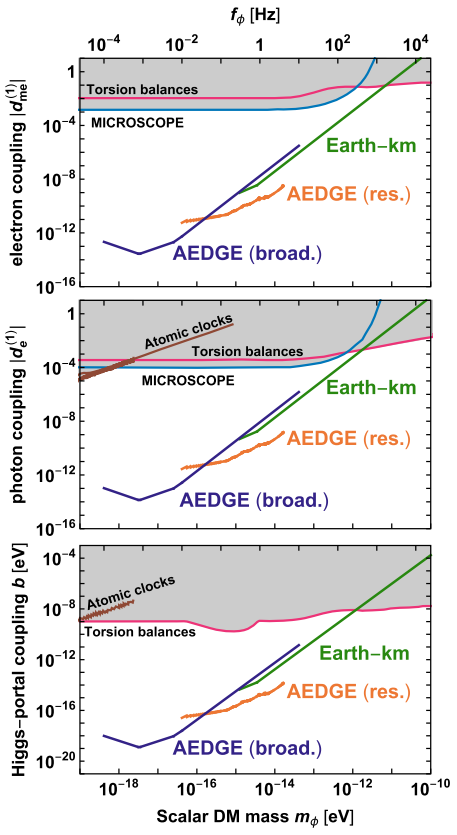


Figure 1 The sensitivities of AEDGE in broadband (purple lines) and resonant mode (orange lines) to linear scalar DM interactions with electrons (top), photons (middle) and via the Higgs portal (bottom), compared to those of a km-scale terrestrial experiment (green lines). The grey regions show parameter spaces that have been excluded by the MICROSCOPE experiment (blue lines) [24, 25], searches for violations of the equivalence principle with torsion balances (red lines) [26, 27], or by atomic clocks (brown lines) [28, 29]

We consider first scenarios where scalar DM couples *linearly* to the Standard Model fields [22, 23] through an interaction of the form

$$\mathcal{L}_{\rm int}^{\rm lin} \supset -\phi\sqrt{4\pi G_{\rm N}}\left[d_{me}^{(1)} m_e \bar{e}e - \frac{d_e^{(1)}}{4} F_{\mu\nu}F^{\mu\nu}\right] + b\phi|H|^2. \tag{3.1}$$

Figure 1 shows the projected sensitivity of AEDGE for three scenarios: light scalar DM with a coupling $d_{me}^{(1)}$ to electrons (top), a coupling $d_e^{(1)}$ to photons (middle), and a Higgs-portal coupling b (bottom). The coloured lines show the couplings that can be detected at signal-to-noise (SNR) equal to one after an integration time of 10^8 s. We show predictions for AEDGE operating in broadband (purple lines) and resonant mode (orange lines) with the sensitivity parameters given in Table 1 below.

The sensitivity of AEDGE in broadband mode extends from $\sim 10^2$ down to $\sim 10^{-4}$ Hz, which is the approximate frequency where gravity gradients become more important than shot noise [19]. Also shown for comparison are the sensitivities of a km-scale ground-based interferometer scenario.[b] The grey regions show parameter space that has already been excluded by the indicated experiments. We see that AEDGE will probe extensive new regions of parameter space for the electron coupling, extending down to $\sim 10^{-14}$ for a scalar mass $\sim 10^{-17}$ eV, and similarly for a photon coupling, while the sensitivity to a Higgs-portal coupling would extend down to 10^{-19} eV for this mass. We see also that the sensitivities of AEDGE would extend to significantly lower masses and couplings than a possible km-scale terrestrial experiment, used here as a benchmark. Figure 1 also shows that when

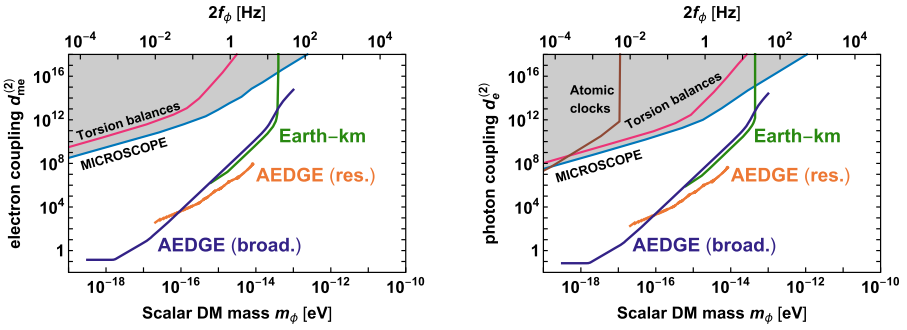


Figure 2 The sensitivities of AEDGE in broadband (purple lines) and resonant mode (orange lines) to quadratic scalar DM interactions with electrons (left) and photons (right), compared to those of a km-scale terrestrial experiment (green lines). The grey regions show parameter spaces that have been excluded by the MICROSCOPE experiment (blue lines) [24, 25], searches for violations of the equivalence principle with torsion balances (red lines) [26, 27], or by atomic clocks (brown lines) [28, 29]

operated in resonant mode AEDGE will have extended sensitivity between 10^{-16} eV and 10^{-14} eV: see Ref. [19] for further details.

Figure 2 illustrates AEDGE capabilities in a scenario where scalar DM couples *quadratically* to Standard Model fields [30]:

$$\mathcal{L}_{\rm int}^{\rm quad} \supset -\phi^2 \cdot 4\pi G_{\rm N} \cdot \left[d_{me}^{(2)} m_e \bar{e} e + \frac{d_{\rm e}^{(2)}}{4} F_{\mu\nu} F^{\mu\nu} \right]. \tag{3.2}$$

Limits and sensitivities to the quadratic coupling $d_{me}^{(2)}$ of scalar DM to electrons are shown in the left panel of Fig. 2, and those for a quadratic coupling $d_e^{(2)}$ to photons in the right panel.[c] As in Fig. 1, the coloured lines show the couplings that can be detected at SNR equal to one for AEDGE operating in broadband (purple lines) and resonant mode (orange lines). We see that AEDGE will also probe extensive new regions of parameter space for the electron and photon quadratic couplings, extending the sensitivity to values of $d_{me}^{(2)}$ and $d_e^{(2)}$ by up to eight orders of magnitude. The quadratic couplings give rise to a richer phenomenology than that offered by linear couplings. For example, a screening mechanism occurs for positive couplings, which reduces the sensitivity of terrestrial experiments [25]. This is illustrated in Fig. 2 by the steep rises in the atomic clock constraints and the sensitivity of a km-scale ground-based interferometer. By comparison, space-based experiments are less affected by the screening mechanism and AEDGE therefore maintains sensitivity at larger masses.

As outlined in [18], AEDGE could also be sensitive to additional ranges of scalar DM masses via direct accelerations of the atoms produced by interactions with dark matter fields, and also through the indirect effects of the inertial and gravitational implications of the variations of the atomic masses and the mass of the Earth. It is estimated that several orders of magnitude of additional unexplored phase space for DM couplings in the mass range of $\sim 10^{-2}$ eV to $\sim 10^{-16}$ eV could be probed via these new effects.

3.1.2 Axion-like particles and vector dark matter

In addition to scalar dark matter, atom interferometers can search for other ultra-light DM candidates.

- Axion-like DM causes the precession of nuclear spins around the axion field. Using atomic isotopes with different nuclear spins, atom interferometers are sensitive to the axion-nucleon coupling for axion-like DM lighter than 10^{-14} eV [31].
- Two interferometers running simultaneously with two different atomic species act as an accelerometer. This set-up is sensitive to, for instance, a dark vector boson with a mass below 10^{-15} eV coupled to the difference between baryon number (B) and lepton number (L) [32].

3.1.3 Identifying a DM signal

Confirming that the origin of a positive detection is due to a DM signal may be challenging. However, there are a number of characteristic features of the DM signal that should allow it to be distinguished from other sources. For example, compared to GW signals from binary systems, where the frequency changes as the binary system evolves, the frequency of the DM signal is set by the mass of the scalar DM and will therefore remain constant. The DM speed distribution may also have distinctive features (see e.g., [33]) and there is a characteristic modulation over the course of a year, caused by the rotation of the Earth about the Sun [34]. If these distinctive features can be measured, they would point to a DM origin for the signal.

3.2 Gravitational waves

The first direct evidence for gravitational waves (GWs) came from the LIGO/Virgo discoveries of emissions from the mergers of black holes (BHs) and of neutron stars [35]. These discoveries open new vistas in the exploration of fundamental physics, astrophysics and cosmology. Additional GW experiments are now being prepared and proposed, including upgrades of LIGO [3] and Virgo [4], KAGRA [5], INDIGO [6], the Einstein Telescope (ET) [7, 8] and Cosmic Explorer (CE) [9], which will provide greater sensitivities in a similar frequency range to the current LIGO and Virgo experiments, and LISA [36], which will provide sensitivity in a lower frequency band on a longer time-scale. In addition, pulsar timing arrays provide sensitivity to GWs in a significantly lower frequency band [37].

As we discuss in more detail below, there are several terrestrial cold atom experiments that are currently being prepared, such as MIGA [38], ZAIGA [39] and MAGIS [40], or being proposed, such as ELGAR [41] and AION [42]. These experiments will provide measurements complementary to LISA and LIGO/Virgo/KAGRA/INDIGO/ET/CE via their sensitivities in the mid-frequency range between 1 and 10^{-2} Hz.

AEDGE will subsequently provide a significantly extended reach for GWs in this frequency range, as we illustrate in the following with examples of astrophysical and cosmological sources of GWs, which open up exciting new scientific opportunities.

3.2.1 Astrophysical sources

The BHs whose mergers were discovered by LIGO and Virgo have masses up to several tens of solar masses. On the other hand, supermassive black holes (SMBHs) with masses $>10^6$ solar masses have been established as key ingredients in most if not all galaxies [43], and play major roles in cosmological structure formation and determining the shape, appearance and evolution of galaxies [44]. A first radio image of the SMBH in M87 has been released by the Event Horizon telescope (EHT) [45], and observations of the Sgr A* SMBH at the centre of our galaxy are expected shortly. The LISA frequency range is ideal for observations of mergers of SMBHs.

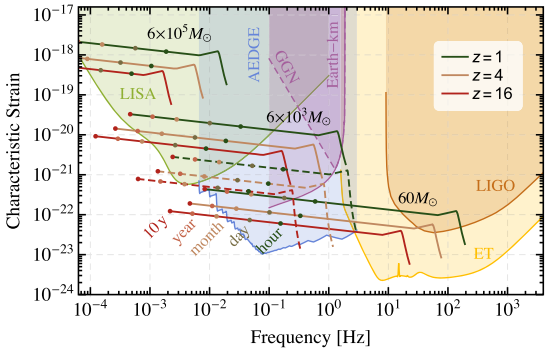


Figure 3 Comparison of the strain measurements possible with AEDGE and other experiments, showing their sensitivities to BH mergers of differing total masses at various redshifts z, indicating also the time remaining before the merger. The solid lines correspond to equal mass binaries and the dashed ones to binaries with very different masses, namely $3000M_\odot$ and $30M_\odot$. Also shown is the possible gravitational gradient noise (GGN) level for a km-scale terrestrial detector, which would need to be mitigated for its potential to be realized. This figure illustrates the potential for synergies between AEDGE and detectors observing other stages of BH infall and merger histories

However, the formation and early evolution of SMBHs [46] and their possible connections to their stellar mass cousins are still among the major unsolved puzzles in galaxy formation. It is expected that intermediate-mass black holes (IMBHs) with masses in the range 100 to 10^5 solar masses must also exist, and there is some observational evidence for them [47]. They may well have played key roles in the assembly of SMBHs. Detecting and characterising the mergers of IMBHs with several hundred to a hundred thousand solar masses will provide evidence whether (and how) some of the most massive "stellar" black holes eventually grow into SMBHs [48] or whether SMBHs grow from massive seed black holes formed by direct collapse from gas clouds in a subset of low-mass galaxies [49, 50].

The AEDGE frequency range between $\sim 10^{-2}$ and a few Hz, where the LISA and the LIGO/Virgo/KAGRA/INDIGO/ET/CE experiments are relatively insensitive, is ideal for observations of mergers involving IMBHs, as seen in Fig. 3. This figure shows that AEDGE (assumed here to be operated in resonant mode) would be able to observe the mergers of 6×10^3 solar-mass black holes out to very large redshifts z, as well as early inspiral stages of mergers of lower-mass BHs of $60M_\odot$, extending significantly the capabilities of terrestrial detectors to earlier inspiral stages. The dashed lines illustrate the observability of binaries with very different masses, namely $3000M_\odot$ and $30M_\odot$, which could be measured during inspiral, merger and ringdown phases out to large redshifts.[d]

The left panel of Fig. 4 shows the sensitivity of AEDGE operating in resonant mode for detecting GWs from the mergers of IMBHs of varying masses at various signal-to-noise (SNR) levels $\geq$5. It could detect mergers of $\sim 10^4$ solar-mass BHs with SNR $\gtrsim 1000$ out to $z \sim 10$, where several dozen such events are expected per year according to [51], and mergers of $\sim 10^3$ solar-mass BHs with SNR $\gtrsim 100$ out to $z \gtrsim 100$. Such sensitivity should be sufficient to observe several hundred astrophysical BH mergers according to [51]. This paper suggests that such events would be expected in the smaller part of this redshift range, so the observation of additional mergers at large redshifts could be a distinctive signature of primordial BHs.

Another astrophysical topic where AEDGE can make a unique contribution is whether there is a gap in the spectrum of BH masses around $200M_\odot$. We recall that electron-

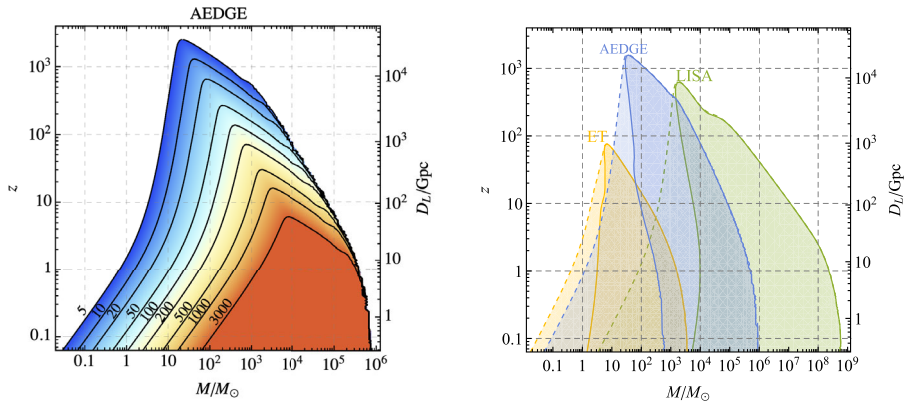


Figure 4 Left panel: The sensitivity of AEDGE to the mergers of IMBHs with the contours showing the signal-to-noise ratio (SNR). Right panel: Comparison of the sensitivities of AEDGE, ET and LISA with threshold SNR = 8. In the lighter regions between the dashed and solid lines the corresponding detector observes only the inspiral phase

positron pair-instability is calculated to blow apart low-metallicity stars with masses around this value, leaving no BH remnant (see, for example, [52]). The AEDGE frequency range is ideal for measuring the inspirals of BHs with masses $\sim 200 M_\odot$ prior to their mergers. If they are observed, such BHs might be primordial, or come from higher-metallicity progenitors that are not of Population III, or perhaps have been formed by prior mergers.

In addition to the stand-alone capabilities of AEDGE illustrated in Figs. 3 and 4, there are significant synergies between AEDGE measurements and observations in other frequency ranges, like those proposed in [53] for the synergistic operation of LISA and LIGO:

- The measurement of early inspiral stages of BH-BH mergers of the type discovered by LIGO and Virgo is guaranteed science for AEDGE. As seen in Fig. 3, AEDGE would observe out to high redshifts early inspiral stages of such mergers, which could subsequently be measured weeks or months later by LIGO/Virgo/KAGRA/INDIGO/ET/CE. The inspiral phases of these sources could be measured for a month or more by AEDGE, enabling the times of subsequent mergers to be predicted accurately. The motion of the detectors around the Sun as well as in Earth orbit would make possible the angular localization with high precision of the coming merger [54], providing 'early warning' of possible upcoming multimessenger events. The right panel of Fig. 4 compares the sensitivities of AEDGE at the SNR = 8 level (blue shading) with that of ET (yellow shading). The overlaps between the sensitivities show the possibilities for synergistic observations, with AEDGE measuring GWs emitted during the inspiral phase (lighter shading), and ET subsequently observing infall, the merger itself and the following ringdown phase (darker shading).

  Figure 5 shows some examples of these possible synergies for AEDGE measurements of the inspiral phases of binaries that merge in the LIGO/Virgo sensitivity window. The upper left plot shows the SNR as a function of redshift, and the other plots show how precisely various observables can be measured by observing for 180 days before the frequency of the signal becomes higher than 3 Hz, corresponding to the upper limit of the AEDGE sensitivity window. As examples, we see in the upper middle panel that for events typical of those observed by LIGO/Virgo

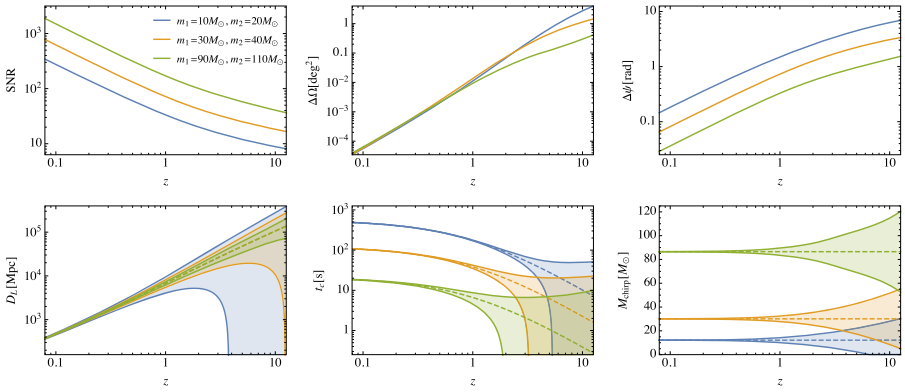


Figure 5 The SNR (upper left panel), the sky localization uncertainty $\Delta\Omega$ (upper middle panel), the polarization uncertainty $\Delta\psi$ (upper right panel), and the uncertainties in the luminosity distance D_L (lower left panel), the time remaining before merger t_c (lower middle panel) and the chirp mass $M_{\rm chirp}$ (lower right panel), calculated for three merging binaries of different BH mass combinations as functions of their redshifts

at $z \simeq 0.1$ the AEDGE sky localization uncertainty is less than 10^{-4}deg^2, while the upper right panel shows that the GW polarization could be measured accurately. The lower middle panel shows that the times of the mergers could be predicted with uncertainties measured in minutes, permitting advance preparation of comprehensive multimessenger follow-up campaigns. We also see in the lower panels that for binaries at high redshifts $z \gtrsim 1$ the uncertainties in the luminosity distance, the time before merger and the chirp mass become significant, though in these cases the measurements could be improved by starting to observe the binary more than 180 days before it exits the sensitivity window.

- Conversely, as also seen in Fig. 3 and the right panel of Fig. 4, operating AEDGE within a few years of LISA would provide valuable synergies, as LISA observations of inspirals (lighter green shading) could be used to make accurate predictions for subsequent detections by AEDGE of the infall, merger and ringdown phases of IMBHs in the $\mathcal{O}(10^3 - 10^4)$ solar-mass range (darker blue shading). This is similar to the strategy proposed in [53] for the synergistic operation of LISA and LIGO.
- As discussed in [55], combined measurements by AEDGE and other detectors would provide unparalleled lever arms for probing fundamental physics by measuring post-Newtonian and post-Minkowskian [56] gravitational parameters, probing Lorentz invariance in GW propagation and the possibility of parity-violating gravity.

In summary, the mid-frequency GW detection capabilities of AEDGE discussed here will play a crucial part in characterising the full mass spectrum of black holes and their evolution, thereby casting light on their role in shaping galaxies.[e]

3.2.2 Cosmological sources

- Many extensions of the Standard Model (SM) of particle physics predict first-order phase transitions in the early Universe. Examples include extended electroweak sectors, effective field theories with higher-dimensional operators and hidden-sector interactions. Extended electroweak models have attracted particular interest by providing options for electroweak baryogenesis and magnetogenesis: see, e.g., [57],

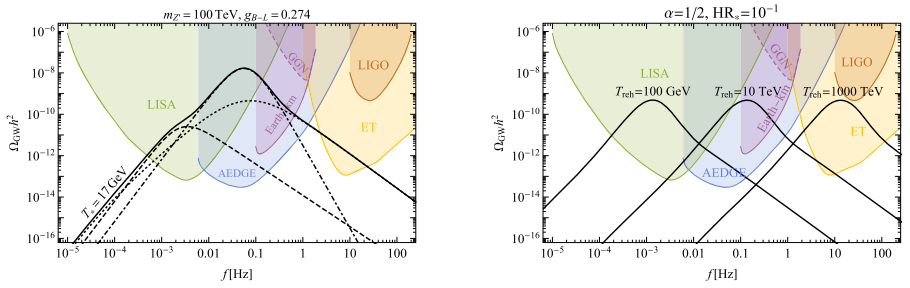


Figure 6 Left panel: Example of the GW spectrum in a classical scale-invariant extension of the SM with a massive Z' boson, compared with various experimental sensitivities. The dashed line shows the contribution to the spectrum sourced by bubble collisions, the dot-dashed line shows the contribution from sound waves, and the dotted line shows the contribution from turbulence. Right panel: Examples of spectra with some other reheating temperatures after the transition that may be realized in the same model

and offer opportunities for correlating cosmological observables with signatures at particle colliders [58, 59].

The left panel of Fig. 6 shows one example of the GW spectrum calculated in a classically scale-invariant extension of the SM with a massive Z' boson, including both bubble collisions and the primordial plasma-related sources [59]. These contributions yield a broad spectrum whose shape can be probed only by a combination of LISA and a mid-frequency experiment such as AEDGE, which is assumed here to be operated at a set of $\mathcal{O}(10)$ resonant frequencies, whose combined data would yield the indicated sensitivity to a broad spectrum. A crucial feature in any model for a first-order phase transition in the early universe is the temperature, T_*, at which bubbles of the new vacuum percolate. For the model parameters used in the left panel of Fig. 6, $T_* = 17$ GeV. The GW spectra for parameter choices yielding various values of the reheating temperature, $T_{\rm reh}$, which are typically $\mathcal{O}(m_{Z'})$ in this model, are shown in the right panel of Fig. 6. We see that AEDGE would play a key role, fixing the parameters of this classically scale-invariant extension of the SM.

Figure 7 shows the discovery sensitivity of AEDGE in the parameter space of the classically scale-invariant extension of the SM with a massive Z' boson. We see that AEDGE could measure a signal from a strong phase transition with high signal-to-noise ratio (SNR) all the way down to the present lower limit of a few TeV on the Z' mass from experiments at the LHC, and covering the mass range where such a boson could be discovered at a future circular collider [60]. The SNR is calculated assuming five years of observation time divided between 10 resonance frequencies, whose data are combined.

- Other possible cosmological sources of GW signals include cosmic strings. As seen in the left panel of Fig. 8, these typically give a very broad frequency spectrum stretching across the ranges to which the LIGO/ET, AEDGE, LISA and SKA [61] experiments are sensitive. The current upper limit on the string tension $G\mu$ is set by pulsar timing array (PTA) measurements at low frequencies [37]. LISA will be sensitive to $G\mu = 10^{-17}$, while AEDGE and ET could further improve on this sensitivity by an order of magnitude. This panel also shows (dashed lines) the impact of including the change in the number of degrees of freedom predicted in the SM. It is apparent that detailed measurements in different frequency ranges could probe both SM processes

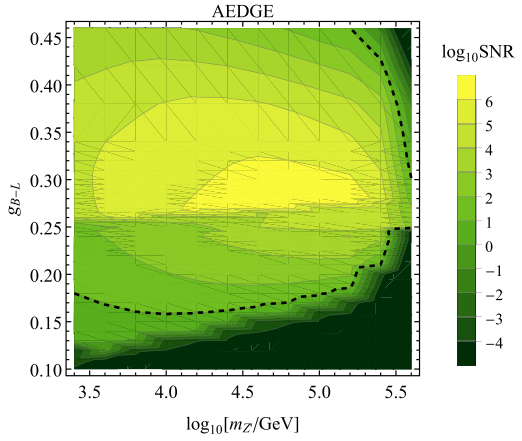


Figure 7 Signal-to-noise ratio (SNR) achievable with AEDGE in the parameter plane of the classically scale-invariant extension of the SM with a massive Z' boson. The dashed line is the SNR = 10 contour

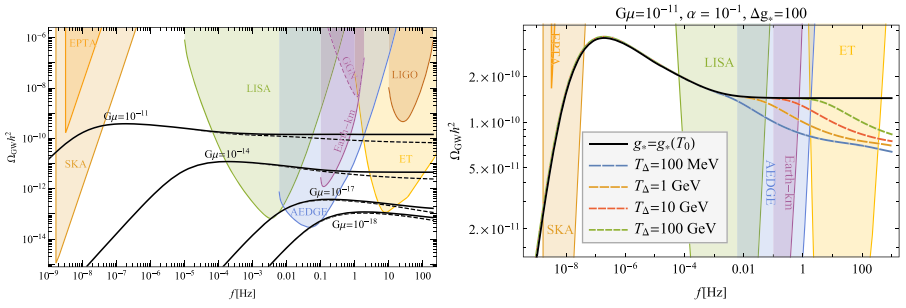


Figure 8 Left panel: Examples of GW spectra from cosmic strings with differing tensions $G\mu$. The dashed lines show the impact of the variation in the number of SM degrees of freedom. Right panel: Detail of the effect on the GW spectrum for the case $G\mu = 10^{-11}$ of a new particle threshold at various energies $T_\Delta \geq 100$ MeV with an increase $\Delta g_* = 100$ in the number of relativistic degrees of freedom

such as the QCD phase transition and BSM scenarios predicting new degrees of freedom, e.g., in a hidden sector, or even more significant cosmological modifications such as early matter domination, which would leave distinguishable features in the GW background. This point is illustrated in the right panel of Fig. 8, where we see the effect on the string GW spectrum of a new particle threshold at energies $T_\Delta \geq 100$ MeV with an increase $\Delta g_* = 100$ in the number of relativistic degrees of freedom. Comparing the string GW strengths at different frequencies at the 1% level would be sensitive to $\Delta g_* = 2$.

In Fig. 9 we show the frequencies at which features would appear in the cosmic string GW spectrum corresponding to events in the early universe occurring at different temperatures. We see that AEDGE would be sensitive in a different range of parameters from ET and LISA. Figures 8 and 9 illustrate that probing the plateau in a wide range of frequencies can provide a significant amount of information not only on strings themselves but also on the early evolution of the universe [62].

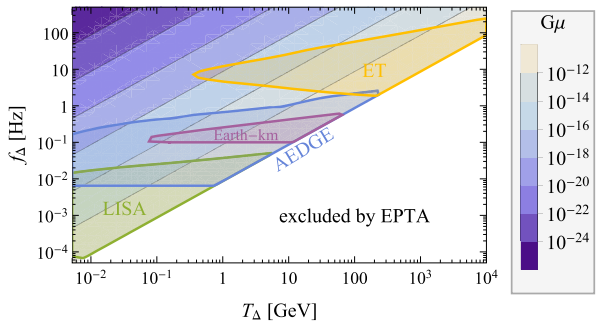


Figure 9 Frequency f_Δ at which features in the cosmic string GW spectrum appear corresponding to events in the early universe occurring at the indicated temperature T_Δ. The shading contours indicate $G\mu$ values of the cosmic string network, and the reach of different experiments are indicated by the coloured regions

3.3 Other fundamental physics

Ultra-high-precision atom interferometry has been shown to be sensitive to other aspects of fundamental physics beyond dark matter and GWs, though studies of some such possibilities are still at exploratory stages. Examples include:

- High-precision measurements of the *gravitational redshift* and quantum probes of the *equivalence principle* [63].
- The possibility of *detecting astrophysical neutrinos* that traverse the Earth with high fluxes though small cross-section: see, e.g., [64]. The great advantage of interferometers in this case is that they are sensitive to very small or even vanishing momentum transfer. Whilst current sensitivities seem far from accessing any interesting background [65], the analyses of this possibility have not been comprehensive.
- *Probes of long-range fifth forces*: Since atom interferometry can be used to detect the gravitational field of Earth [66], a set up with interferometers at different heights seems a natural one to study the possibility of any other long-range fifth force that couples to matter in ways different from gravity. The search for long-range forces is a very active area of research beyond the SM, with natural connections to dark matter and modified gravity, see, e.g., [67], and universally-coupled Yukawa-type fifth forces over these scales are already well constrained by classical searches for fifth forces [68].
- Tests of general relativity: A set-up with atom interferometers at different values of the gravitational potential also facilitates measurements of higher-order general-relativistic corrections to the gravitational potential around the Earth. The leading higher-order effects are due to the gradient of the potential, and corrections due to the finite speed of light, and Döppler shift corrections to the photon frequency.
- *Constraining possible variations in fundamental constants*: A comparison of interferometers at different time and space positions may be useful to test possible variations of fundamental constants in these two domains. There are different motivations for these searches that can be found in [69, 70].
- *Probing dark energy*: The main driver of current cosmological evolution is a puzzling substance that causes the acceleration of the expansion of space-time. This 'dark energy' is supposed to be present locally and one can try to use precise experiments to look for its local effects. This possibility comes in at least two flavours. One can argue that dark energy models naturally involve dynamical ultra-light fields. If the SM is

coupled to them, the fundamental properties of nature would be time- and space-dependent. Another possibility comes from specific models where the dark energy candidate modifies the laws of gravity, where atom interferometry experiments have proved a particularly powerful technique for constraining popular models [71, 72].

- *Probes of basic physical principles*. These include probing Bell inequalities and testing the foundations of quantum mechanics and Lorentz invariance. It has been suggested that some ideas beyond the standard postulates of quantum mechanics (for instance linearity and collapse models) may be tested with precise interferometry of quantum states, see, e.g., [73–76], and atom interferometers have been proposed as test of Lorentz invariance and gravitation in [77].

4 Experimental considerations

In this Section we describe a conceptual detector design that can accomplish the science goals outlined in this document. This basic design requires two satellites operating along a single line-of-sight and separated by a long distance. The payload of each satellite will consist of cold atom technology as developed for state-of-the-art atom interferometry and atomic clocks. For the science projections presented here, we assume a minimum data-taking time of 3 years, which requires a mission duration of at least 5 years, while 10 years would be an ultimate goal.

As two satellites are needed to accomplish its science goals, the AEDGE mission planning costs are estimated to be in the range of an L-class mission. However, in view of the international interest in the AEDGE science goals, the possibility of international cooperation and co-funding of the mission may be investigated.

4.1 Representative technical concept

As we discuss in Sect. 5, there are several cold atom projects based on various technologies that are currently under construction, planned or proposed, which address the principal technical challenges and could be considered in a detailed design for a mission proposal and corresponding satellite payload. However, all of these options require the same basic detector and mission configuration outlined above. For the option presented in this White Paper we have chosen to base our discussion on the concept outlined in [40, 63, 78, 79], which is currently the most advanced design for a space mission.

This concept links clouds of cold atomic strontium in a pair of satellites in medium earth orbit (MEO) via pulsed continuous-wave lasers that induce the 698 nm atomic clock transition, and detect momentum transfers from the electromagnetic field to the strontium atoms, which act as test masses in the double atom interferometer scheme illustrated in Fig. 10. The lasers are separated by a large distance L, the paths of the light pulses are shown as wavy lines, and the atom interferometers, which are represented by the two diamond-shaped loops on an enlarged scale, are operated near them. Laser pulses transfer momenta $\hbar k$ to the atoms and toggle them between the ground state and the excited state. Thus they act as beam splitters and mirrors for the atomic de Broglie waves, generating a quantum superposition of two paths and then recombining them. As in an atomic clock, the phase shift recorded by each atom interferometer depends on the time spent in the excited state, which is related directly to the light travel time across the baseline, namely L/c.

A single interferometer of the type described here, e.g., the interferometer at position x_1 in Fig. 10, would be sensitive to laser noise, but a crucial experiment has demonstrated [80]

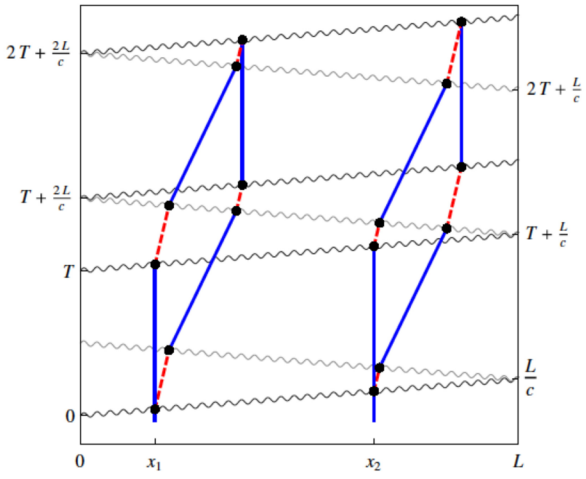


Figure 10 Space-time diagram of the operation of a pair of cold-atom interferometers based on single-photon transitions between the ground state (blue) and the excited state (red dashed). The laser pulses (wavy lines) travelling across the baseline from opposite sides are used to divide, redirect, and recombine the atomic de Broglie waves, yielding interference patterns that are sensitive to the modulation of the light travel time caused by DM or GWs (from [78]). For clarity, the sizes of the atom interferometers are shown on an exaggerated scale

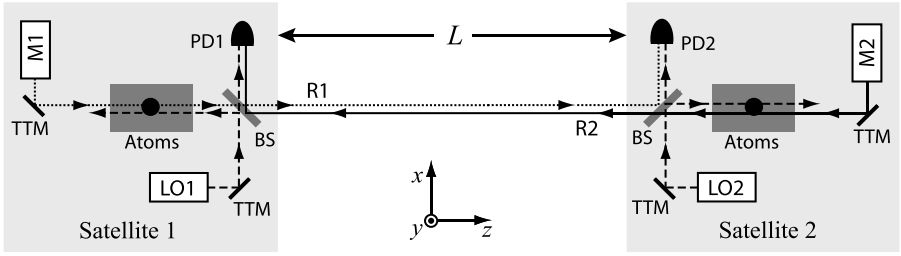


Figure 11 Possible experimental scheme. The beams of the two master lasers M1 and M2 are shown as dotted and solid lines, respectively, together with the corresponding reference beams between the satellites, R1 and R2. Two local oscillator lasers LO1 and LO2 (dashed lines) are phase-locked with R2 and R1, respectively. Photodetectors PD1 and PD2 measure the heterodyne beatnote between the reference beams R2 and R1 and the corresponding local lasers LO1 and LO2, respectively, providing feedback for the laser link. Non-polarizing beam splitters are denoted by BS, and tip-tilt mirrors used for controlling the directions of the laser beams are denoted by TTM. For clarity, small offsets between overlapping laser beams have been introduced. Figure taken from [40]

that this can be substantially suppressed by the differential measurement between the two interferometers at x_1 and x_2 as suggested in [78]. The sensitivity of a single such interferometer could be substantially improved in the two-interferometer configuration outlined here by measuring the differential phase shift between the widely-separated interferometers [78]. The GW (or DM) signal provided by the differential phase shift is proportional to the distance L between the interferometers, whereas the laser frequency noise largely cancels in the differential signal.

Based on this approach using two cold-atom interferometers that perform a relative measurement of differential phase shift, we propose a mission profile using a pair of satellites similar to that used for atomic gravity gradiometers [81, 82], which is shown in Fig. 11. As the atoms serve as precision laser frequency references, only two satellites operating

along a single line-of-sight are required to sense gravitational waves. The satellites both contain atom interferometers that are connected by laser pulses propagating along the positive and negative z directions in the diagram, and the clouds of ultracold atoms at the ends of the baseline of length L act as inertial test masses. There are intense master lasers (M1 and M2) in the satellites, which drive the atomic transitions in the local atom interferometers. After interaction with the atoms, each master laser beam is transmitted by the beam splitter (BS) out of the satellite, and propagates towards the other satellite, and R1 and R2 are beams from satellite 1 and 2, respectively, that play the roles of reference beams.

Intense local lasers LO1 and LO2 are used to operate the atom interferometers at each end of the baseline. These otherwise independent local lasers are connected by reference laser beams R1 and R2 that are transmitted between the two spacecraft, and the phases of the local lasers are locked/monitored with respect to the incoming wavefronts of these reference lasers, as illustrated in Fig. 11. A detailed description is available in [40, 79, 83].

In addition to photodetectors PD1 and PD2 for measuring the phase differences between the two beams in both satellites, the spatial interference patterns are characterized by quadrant detectors (or cameras), enabling the pointing directions and spatial modes of the two lasers to be well matched using appropriate feedback. Feedback applied to the tip-tilt mirrors (TTMs) in Fig. 11 can then be used to control the angles of the local lasers. Similarly, the angle of the master laser itself can be controlled by comparing it to the local laser direction and using another TTM.

With satellites in MEO, the measurement baseline re-orients on a time scale that is short compared to the expected duration of the GW signals from many anticipated sources. This allows efficient determination of the sky position and can provide polarization information. The relatively short measurement baseline, compared to LISA, provides good sensitivity in the 0.01 Hz to 1 Hz frequency band, intermediate between the LISA and LIGO antenna responses, and suited to GW astronomy, cosmology and DM searches, as described above.

4.2 Sensitivity projections

In order to establish sensitivity estimates for the different physics goals described above, we have to choose a concrete scenario and define quantitative projections.

For example, a GW would modify the light travel time across the baseline of the two-satellite system, varying the time spent in the excited state by atoms at each end of the baseline, generating a differential phase shift between the two atom interferometers. The phase response of the detector can be written as $\Delta\Phi_{\rm grad}(t_0) = \Delta\phi\cos(\omega t_0 + \phi_0)$, where $\omega t_0 + \phi_0$ is the phase of the GW at time t_0 at the start of the pulse sequence. The resulting amplitude of the detector response is [79]:

$$\Delta\phi = k_{\rm eff} hL \frac{\sin(\omega QT)}{\cos(\omega T/2)} \operatorname{sinc}\left(\frac{\omega nL}{2c}\right) \sin\left(\frac{\omega T}{2} - \frac{\omega(n-1)L}{2c}\right), \tag{4.1}$$

where $\hbar k_{\rm eff}$ is the effective momentum transfer, and $k_{\rm eff} \equiv n\omega_A/c$ for an n-pulse sequence generating an atomic transition with level spacing $\hbar\omega_A$. The response (4.1) is peaked at the resonance frequency $\omega_r \equiv \pi/T$ and exhibits a bandwidth $\sim \omega_r/Q$. The amplitude of

the peak phase shift on resonance is

$$\Delta\phi_{\rm res} = 2Qk_{\rm eff}hL\,\mathrm{sinc}\left(\frac{\omega_r nL}{2c}\right)\cos\left(\frac{\omega_r(n-1)L}{2c}\right), \tag{4.2}$$

which reduces in the low-frequency limit $\omega_r \ll \frac{c}{nL}$ to $\Delta\phi_{\rm res} \approx 2Qk_{\rm eff}hL$. The phase response shows an n-fold sensitivity enhancement from large momentum transfer (LMT). The interferometer can be switched from broadband to resonant mode by changing the pulse sequence used to operate the device (changing Q) [79], resulting in a Q-fold enhancement.

For the sensitivity projections of AEDGE presented in this paper we assume that operation is performed mainly in the resonant mode, while also providing estimates for broadband operation for comparison. In order to generate the sensitivity curve for, e.g., a GW signal, from the phase response, we calculate the minimum strain h that is detectable given a phase noise spectral density $\delta\phi_{\rm noise}$. We optimize the LMT enhancement n for each frequency and resonant enhancement Q, taking into account the detector design constraints, which include the limits on the total number of pulses, $n_p^{\rm max} = 2Q(2n-1)+1$, and on the maximum interferometer duration, $2TQ < T_{\rm int}$, where $T_{\rm int}$ is the time over which the atom interferometer is interrogated. Furthermore, as we assume in the design outlined above that the interrogation region of the atoms is placed within the satellite, the wavepacket separation $\Delta x = \hbar k_{\rm eff}(T/m)$, where m is the atom mass, is constrained to be less than 90 cm. As discussed in [40, 79], this constraint limits the amount of LMT enhancement. Using resonant enhancement while reducing LMT allows the interferometer region to remain small, but it has an impact on the achievable sensitivity when setup is operated in broadband mode. In this context, we would like to point out that a strontium-based single-photon atom interferometer has recently demonstrated 141 $\hbar k$ LMT [84]. Although the demonstrated LMT does not yet reach the performance requirements for proposed ground-based detectors or AEDGE, it serves as a proof-of-principle for future LMT-enhanced clock atom interferometry for dark matter searches and gravitational wave detection. Planned improvements of this work, like significantly increased laser power, are expected to push the LMT transfer rate to about 1000 $\hbar k$ in the near future, which would reach the conceptual design specification of AEDGE. An alternative design places the interrogation region outside the satellite [85]. This setup would support LMT values closer to what can be achieved in ground-based setups, which would not only increase broadband sensitivity but also make it possible to probe even lower frequencies. However, operating the interferometers in space would incur additional technical challenges such as vacuum stability, solar radiation shielding and magnetic field effects. While these challenges seem surmountable, conservatively we focus our sensitivity projections here on a design in which the atom interrogation region is within the satellite, which requires resonant mode operation to achieve maximal sensitivity. In the future, further investigations of using a much larger interrogation region in space could change this design choice.

This resonant mode strategy provides significant sensitivity to a stochastic background of gravitational waves, e.g., of cosmological origin. To indicate the sensitivity estimates for the density of GW energy, $\Omega_{\rm GW}$, we use power-law integration [86] to display an envelope of power-law signals for each given frequency detectable with an assumed SNR = 10. In the calculation for AEDGE we assume five years of observation time divided between 10 logarithmically-distributed resonance frequencies and sum the signal from the total

Table 1 List of basic parameters of strontium atom interferometer designs for AEDGE and a benchmark 1-km terrestrial experiment using similar technologies: length of the detector L; interrogation time of the atom interferometer $T_{\rm int}$; phase noise $\delta\phi_{\rm noise}$; and the total number of pulses $n_p^{\rm max}$, where n is the large momentum transfer (LMT) enhancement and Q the resonant enhancement. The choices of these parameters predominately define the sensitivity of the projection scenarios [40]

Sensitivity scenario	L [m]	$T_{\rm int}$ [sec]	$\delta\phi_{\rm noise}$ [$1/\sqrt{\rm Hz}$]	$n_p^{\rm max}=2Q(2n-1)+1$ [number]
Earth-km	2000	5	0.3×10^{-5}	40,000
AEDGE	4.4×10^{7}	300	10^{-5}	1000

running time of the experiment. We have verified that changing this scanning strategy by using a different number of resonant frequencies does not have a strong impact on the resulting sensitivity. These curves thus have the property that any power-law signal touching them would give the required SNR in the indicated experiment. For ease of comparison, we also assumed five years of operation for each of the other experiments shown.

The quantitative projections for the DM and GW signals we presented in the previous Sections are based on the following scenarios:

- *Earth-km*: This scenario represents the sensitivity estimate of a terrestrial detector at the km-scale using typical parameters that are projected to be achieved in the future. This sets the benchmark for comparison with the space-based AEDGE.
- *AEDGE*: This scenario represents the sensitivity estimate of a space-based detector using parameters that could be achieved for this set-up. This sets the benchmark for the sensitivity of space-based detector proposed in this White Paper.

The values of the basic parameters assumed for the different sensitivity scenarios are listed in Table 1. These parameters dominate in determining the sensitivities for the DM and GW projections presented in Sects. 3.1 and 3.2, respectively.

5 Technological readiness

AEDGE will benefit from the experience gained with LISA Pathfinder in free-fall control and LISA itself in operating laser interferometers over large distances. We have identified the following three additional high-level technical requirements that are critical for AEDGE:

- Demonstrate reliable functioning of atom interferometry on a large terrestrial scale $\gtrsim$100 m.
- Demonstrate that the design parameters assumed here, such as the LMT enhancement, phase noise control, interrogation time, etc., can be achieved.
- Demonstrate the robustness of cold atom technology in the space environment.

Several terrestrial atom interferometer projects that would serve as demonstrators for different technologies are under construction, planned or proposed, representing a qualitative change in the state of technological readiness since the SAGE project [63] was reviewed by ESA in 2016. As described below, they should be able to show how the above-mentioned technical requirements can be met and demonstrate TRL5 technology readiness (according to ISO Standard 16290).

- Three large-scale prototype projects at the 100-m scale are funded and currently under construction, namely MAGIS-100 in the US, MIGA in France, and ZAIGA in China. These will demonstrate that atom interferometry at the large scale is possible,

paving the way for terrestrial km-scale experiments. Assuming that large-scale prototyping is successful within five years, extending the technology to the km scale will be the next step. There are projects to build one or several more km-scale detectors in the US (at the Sanford Underground Research facility, SURF), in Europe (MAGIA-advanced, ELGAR) and in China (advanced ZAIGA) that would serve as the ultimate technology readiness demonstrators for AEDGE. It is foreseen that by about 2035 one or more km-scale detectors will have entered operation.

- In parallel to these large-scale prototype projects, several other cold atom projects are in progress or planned, demonstrating the general readiness of the technology including the scaling of the basic parameters that are required for AEDGE. In fact, the basic requirements for AEDGE in terms of atom interferometry are more relaxed than those one of the km-scale terrestrial detectors, as the main sensitivity driver for AEDGE will be the long baseline, and its requirements for the basic parameters of atom interferometry are less stringent than in the km-scale projects.
- Several cold atom experiments (CACES [87], MAIUS [88], CAL [89]) and underlying optical key technologies (FOKUS [90], KALEXUS [91], JOKARUS [92]) have already demonstrated reliable operation in space, and much more experience will be gained in the coming years.

We now summarize the statuses of some of the key "AEDGE pathfinder" experiments:

- The Matter-wave laser Interferometric Gravitation Antenna (MIGA) experiment [38], a double 150-m-long optical cavity in Rustrel, France is fully funded and currently in the final phase of construction. MIGA aims at demonstrating precision measurements of gravity with cold atom sensors in a large-scale instrument and at studying associated applications in geoscience and fundamental physics. MIGA will employ an array of atom interferometers along the same optical link to mitigate the main noise contribution at low frequency represented on Earth by Newtonian noise [93]. In particular, it will assess future potential applications of atom interferometry to gravitational wave detection in the mid-frequency band between $\sim$0.1 and 10 Hz intermediate between LISA and LIGO/Virgo/KAGRA/INDIGO/ET/CE.
- The MAGIS project [40] in the US plans a series of interferometers using cold atoms with progressivly increasing baselines of $\sim$10 m, $\sim$100 m, and $\sim$1 km. The first step is funded and under construction at Stanford, the second step is also funded and being prepared at Fermilab, and the third step is planned for a km-scale vertical shaft at SURF.
- The Zhaoshan long-baseline Atom Interferometer Gravitation Antenna (ZAIGA) is an underground laser-linked interferometer facility [39] under construction near Wuhan, China. It has an equilateral triangle configuration with two atom interferometers separated by a km in each arm, a 300-meter vertical shaft equipped with an atom fountain and atomic clocks, and 1-km-arm-length optical clocks linked by locked lasers. It is designed for a comprehensive range of experimental research on gravitation and related problems including GW detection and high-precision tests of the equivalence principle.
- Building upon the MAGIA experiment [94, 95], MAGIA-Advanced is an R&D project funded by the Italian Ministry for Research and the INFN for a large-scale atom interferometer based on ultracold rubidium and strontium atoms. In addition to laboratory activity, the team is investigating the possibility of a 100–300 m atom

interferometer to be installed in a vertical shaft in Sardinia. Its main goals are GW observation and the search for DM.

- ELGAR is a European initiative to build a terrestrial infrastructure based on cold atoms for GW detection with potential applications also for other aspects of gravitation and fundamental physics such as DM. ELGAR will use a large scale array of correlated Atom Interferometers. A White Paper about this infrastructure is being prepared [96].
- The AION project in the UK [42] proposes a series of atom interferometers baselines of ∼10 m, ∼100 m, and ∼1 km, similar to MAGIS, with which it will be networked à la LIGO/Virgo. The first stage would be located in Oxford, with sites for the subsequent stages awaiting more detailed study.

The above terrestrial projects will demonstrate various concepts for large-scale cold atom interferometers and provide valuable operational experience. In addition there are ongoing NASA, Chinese, ESA, German and French projects to conduct cold atom experiments in space, some of which have already provided operational experience with cold atoms in space or microgravity environments:

- NASA recently installed the Cold Atom Laboratory (CAL) experiment on the ISS. It is reported that the CAL system has been performing nominally and that rubidium Bose-Einstein condensates (BECs) have subsequently been produced in space on nearly a daily basis [89],[f] and the continuation of the CAL science programme will include an atomic interferometer.
- The Chinese Atomic Clock Ensemble in Space (CACES) demonstrated in-orbit operation of an atomic clock based on laser-cooled rubidium atoms [87].
- The Atomic Clock Ensemble in Space (ACES/PHARAO) project led by ESA plans to install ultra-stable atomic cesium clocks on the ISS, enabling several areas of research including tests of general relativity and string theory, and very long baseline interferometry [97, 98].
- The Bose-Einstein Condensate and Cold Atom Laboratory (BECCAL) is a bilateral project of NASA and the German Aerospace Center (DLR) for a multi-purpose facility on the international space station, based in the heritage of drop-tower (QUANTUS [99]) and sounding-rocket experiments (MAIUS [88]). It will enable a variety of experiments in atom optics and atom interferometery, covering a broad spectrum of research ranging from fundamental physics to studies for applications in earth observation. It is also intended as a pathfinder for future space missions [100].
- The ICE experiment operates a dual-species atom interferometer in weightlessness in parabolic flights [101], and recently reported the all-optical formation of a BEC in the microgravity environment obtained on an Einstein elevator [102].
- In the context of the ISS Space Optical Clock (I-SOC) project of ESA [103, 104] to use cold strontium atoms in space to compare and synchronize atomic clocks worldwide (which can also be used to look for topological DM), ESA is running a development programme aimed at increasing the TRL of strontium-related laser technology. Industrial consortia are currently developing 462 nm and 689 nm lasers, a laser frequency stabilization system, a 813 nm lattice laser, an ultrastable reference cavity and a two-way time/frequency microwave link.

For completeness, we also mention other proposals for atomic experiments in space to probe fundamental physics:

- STE-QUEST is a fundamental science mission that was originally proposed for launch within the ESA Cosmic Vision programme, aimed at probing various aspects of Einstein's theory of general relativity and testing the weak equivalence principle. It features a spacecraft with an atomic clock and an atom interferometer [105]. This mission is also the subject of a Voyage 2050 White Paper.
- Some of the present authors proposed the Space Atomic Gravity Explorer (SAGE) mission to the European Space Agency in 2016 in response to a Call for "New Ideas" [63], with the scientific objectives to investigate GWs, DM and other fundamental aspects of gravity, as well as the connection between gravitational physics and quantum physics, combining quantum sensing and quantum communication based on recent impressive advances in quantum technologies for atom interferometers, optical clocks, microwave and optical links.
- The SagnAc interferometer for Gravitational wavE proposal (also called SAGE) [106] was envisaged to detect GWs with frequency ∼1 Hz using multiple CubeSats on ballistic trajectories in geostationary orbit.
- The Atomic Interferometric Gravitational-Wave Space Observatory (AIGSO) has been proposed in China [107].

AEDGE will also benefit from studies for the Search for Anomalous Gravitation using Atomic Sensors (SAGAS) project [108] and the past Space Atom Interferometer (SAI) project [109, 110], and will maintain contacts with CERN, with a view to applying as a recognized experiment when funded.

6 Summary

The nature of DM is one of the most important and pressing in particle physics and cosmology, and one of the favoured possibilities is that it is provided by coherent waves of some ultra-light boson. As we have illustrated with some specific examples, AEDGE will be able to explore large ranges of the parameter spaces of such models, complementing the capabilities of other experiments.

Experience with electromagnetic waves shows the advantages of making astronomical observations in a range of different frequencies, and the same is expected to hold in the era of gravitational astronomy. There are advanced projects to explore the GW spectrum with maximum sensitivities at frequencies $\gtrsim$10 Hz and below $\lesssim 10^{-2}$ Hz, but no approved project has peak sensitivity in the mid-frequency band between them. As we have discussed, the mergers of intermediate-mass black holes, first-order phase transitions in the early universe and cosmic strings are among the possible GW sources that could produce signals in the mid-frequency band. As we have also discussed, AEDGE would be ideal for exploiting these scientific opportunities, complementing other experiments and offering synergies with them.

Other possible opportunities for AEDGE in fundamental physics, astrophysics and cosmology have been identified, but not yet explored in detail. However, the examples of DM and GWs already indicate that AEDGE offers rich possibilities for scientific exploration and discovery.

The roadmap towards the AEDGE mission includes the following elements:

- Today to 2025: Prototype 10-m facilities in the US, Europe and China, being extended to $\mathcal{O}(100)$ m.
- 2025 to 2035: scaling of 100-m facilities to km-scale infrastructures.

- These experiments will demonstrate the reliability of cold-atom interferometers capable of achieving or surpassing the technical requirements for AEDGE.
- Operation of LISA will demonstrate the operation of large-scale laser interferometry in space.
- In parallel, a vigorous technology development programme should be set up, pursued and coordinated on a European-wide level in order to maximize efficiency and avoid duplication. so as to build on the ground work laid by the development of ACES/PHARAO, the recent demonstration experiments of cold-atom and laser technology on rockets, and the laser technology development currently funded by ESA, and thereby continue the demonstrations by initial US, European and Chinese experiments of the robustness of cold-atom technology in space.

AEDGE is a uniquely interdisciplinary mission that will harness cold atom technologies to address key issues in fundamental physics, astrophysics and cosmology that can be realized within the Voyage 2050 Science Programme of ESA. The worldwide spread of the authors of this article indicate that there could be global interest in participating in this mission.

Acknowledgements
We thank CERN for kindly hosting the workshop where the concept for this proposed experiment was developed.

Funding
Not applicable. The project proposed in this paper is not yet funded.

Abbreviations
ACES/PHARAO, Atomic Clock Ensemble in Space/Projet d'Horloge à Refroidissement d'Atomes en Orbite; AIGSO, Atomic Interferometric Gravitational-Wave Space Observatory; ALIA, Advanced Laser Interferometer Antenna; ALP, Axion-like particle; BEC, Bose–Einsten Condensate; BECCAL, Bose–Einstein Condensate and Cold Atom Laboratory; BS, Beam splitter; CACES, Cold Atom Clock Experiment in Space; CAL, Cold Atom Laboratory; CERN, Conseil Européen pour le Recherche Nucléaire; CMB, Cosmic Microwave Background; DECIGO, Deci-Hertz Interferometer Gravitational Wave Observatory; DLR, Deutsches Zentrum für Luft- und Raumfahrt; DM, Dark Matter; ESA, European Space Agency; FOKUS, Faserlaserbasierter Optischer Kammgenerator unter Schwerelosigkeit; INFN, Istituto Nazionale per la Fisica Nucleare; ICE, atomique à sources Cohérentes pour l'Espace; ISO, International Organization for Standardization; I-SOC, ISS space optical clock; ISS, International Space Station; JOKARUS, Jod Kamm Resonator unter Schwerelosigkeit; KALEXUS, Kalium-Laserexperimente unter Schwerelosigkeit; LMT, Large momentum transfer; MAGIA, Misura Accurata di G mediante Interferometria Atomica; MAIUS, Materiewellen Interferometer Unter Schwerelosigkeit; MEO, Medium earth orbit; MICROSCOPE, Micro-Satellite à traînée Compensée pour l'Observation du Principe d'Equivalence; NASA, National Aeronautics and Space Agency; QUANTUS, Quantengase Unter Schwerelosigkeit; SAGAS, Search for Anomalous Gravitation using Atomic Sensors; SAGE, Space Atomic Gravity Explorer, Sagnac interferometer for gravitational wave; SAI, Space Atom Interferometer; STE-QUEST, Space-Time Explorer and QUantum Equivalence Principle Space Test; SURF, Sanford underground research facility; TRL, Technology readiness level; TTM, Tip-tilt mirror; WIMP, Weakly-Interacting Massive Particle.

Availability of data and materials
Not applicable. For all requests relating to the paper, please contact author Oliver Buchmueller.

Competing interests
The authors declare that they have no competing interests.

Authors' contributions
The author OB is the contact person for this paper. The following authors are the original proponents of a submission in response to the Call for White Papers for the Voyage 2050 long-term plan in the ESA Science Programme: AB, KB, PB, OB, BC, L-IC, MLC, JC, ADR, JE, PWG, MGH, AH, JH, WvK, MK, ML, CMcC, AP, ER, AR, DOS, SS, CS, CS, FS, YS, GMT, VV, M-SZ. All authors discussed the content of the paper and contributed to the writing of the manuscript. All authors read and approved the final manuscript.

Author details
[1]Physics Department, Harvard University, Cambridge, USA. [2]Department of Physics, University of Washington, Seattle, USA. [3]Institute of Physics, Humboldt Universität zu Berlin, Berlin, Germany. [4]Blackett Laboratory, Imperial College London, London, UK. [5]Institute of Physics Belgrade, University of Belgrade, Belgrade, Serbia. [6]Department of Physics, University of Trieste, and Istituto Nazionale di Fisica Nucleare, Trieste Section, Trieste, Italy. [7]Institut für Theoretische Physik, Technische Universität Berlin, Berlin, Germany. [8]LP2N, Laboratoire Photonique, Numérique et Nanosciences, Université Bordeaux-IOGS-CNRS:UMR 5298, Talence, France. [9]Clarendon Laboratory, University of Oxford, Oxford, UK. [10]Department of Theoretical Physics, University of Valencia, and IFIC, Joint Centre Univ. Valencia-CSIC, Valencia, Spain.

[11]Central Laser Facility, STFC - Rutherford Appleton Laboratory, Didcot, UK. [12]Department of Physics, University of Strathclyde, Glasgow, UK. [13]Department of Physics, King's College London, London, UK. [14]Institute of Electronic Structure and Laser, Foundation for Research and Technology-Hellas, Heraklion, Greece. [15]Department of Physics and Astronomy, University of Birmingham, Birmingham, UK. [16]Department of Physics and Astronomy, University College London, London, UK. [17]Department of Physics, University of Liverpool, Liverpool, UK. [18]National Physical Laboratory, Teddington, UK. [19]School of Physics and Astronomy, University of Nottingham, Nottingham, UK. [20]Department of Physics and Astronomy, University of Sussex, Brighton, UK. [21]Institute of Space Science, Ilfov, Romania. [22]Istituto Nazionale di Fisica Nucleare, Sezione di Pisa, Pisa, Italy. [23]University of Crete and Foundation for Research and Technology-Hellas, Heraklion, Greece. [24]Department of Physics, Northern Illinois University, DeKalb, USA. [25]Fermi National Accelerator Laboratory, Batavia, USA. [26]Department of Electronics, Peking University, Beijing, China. [27]Dipartimento di Fisica "Enrico Fermi", Università di Pisa, Pisa, Italy. [28]INFN, Sezione di Pisa, Pisa, Italy. [29]Department of Physics and Astronomy, University of California, Riverside, USA. [30]Department of Physics, University of Nevada, Reno, USA. [31]Antwerp University, Wilrijk, Belgium. [32]Experimental Physics Department, CERN, Geneva, Switzerland. [33]Department of Physics, SEENET-MTP Centre, University of Niš, Niš, Serbia. [34]Particle Physics Department, STFC - Rutherford Appleton Laboratory, Didcot, UK. [35]National Institute of Chemical Physics & Biophysics, Tallinn, Estonia. [36]Theoretical Physics Department, CERN, Geneva, Switzerland. [37]Basic Science Department, Faculty of Engineering, The British University in Egypt (BUE), El Sherouk, Egypt. [38]Physics Department, Faculty of Science, Beni Suef University, Beni Suef, Egypt. [39]University Mohammed V, Rabat, Morocco. [40]School of Mathematical Sciences, University of Nottingham, Nottingham, UK. [41]Institut für Quantenoptik, Leibniz Universität Hannover, Hannover, Germany. [42]LCAR, UMR5589, Université Paul Sabatier, Toulouse, France. [43]SYRTE, Observatoire de Paris, Université PSL, CNRS, Sorbonne Université, LNE, Paris, France. [44]Cavendish Laboratory, University of Cambridge, Cambridge, UK. [45]Department of Physics and Astronomy, Wayne State University, Detroit, USA. [46]Department of Physics, Stanford University, Stanford, USA. [47]Kavli Institute for Cosmology and Institute of Astronomy, Cambridge, UK. [48]Department of Physics and Technology, University of Bergen, Bergen, Norway. [49]GRAPPA, University of Amsterdam, Amsterdam, The Netherlands. [50]Department of Physics and Astronomy, Northwestern University, Evanston, USA. [51]University of Bristol, Bristol, UK. [52]Faculty of Physics, University of Warsaw, Warsaw, Poland. [53]Università di Salerno and Istituto Nazionale di Fisica Nucleare, Napoli, Italy. [54]Department of Physics, University of Illinois at Urbana-Champaign, Urbana, USA. [55]Center for High Energy Physics, Fayoum University, Faiyum, Egypt. [56]Materials Science and Techonology Department, University of Crete, Heraklion, Greece. [57]Queen's University, Belfast, UK. [58]Department of Physics, Brandeis University, Waltham, USA. [59]Dipartimento di Fisica, Università di Bologna, Bologna, Italy. [60]International School of Photonics, Cochin University of Science and Technology, Cochin, India. [61]Institute of Quantum Technologies, German Aerospace Center (DLR), Ulm, Germany. [62]School of Physics and Astronomy, University of Manchester, Manchester, UK. [63]Niels Bohr Institute, University of Copenhagen, Copenhagen, Denmark. [64]Institut für Experimentalphysik, Heinrich-Heine-Universität Düsseldorf, Düsseldorf, Germany. [65]Faculty of Physics, VCQ, University of Vienna, Vienna, Austria. [66]Istituto Nazionale di Fisica Nucleare, Sez. di Genova, Genova, Italy. [67]Physics Department, Florida State University, Tallahassee, USA. [68]Dipartimento di Fisica e Astronomia and LENS, Università di Firenze, Firenze, Italy. [69]Istituto Nazionale di Fisica Nucleare, Firenze, Italy. [70]Department of Physics, University of Illinois at Chicago, Chicago, USA. [71]RAL Space, STFC - Rutherford Appleton Laboratory, Didcot, UK. [72]ZARM, University of Bremen, Bremen, Germany. [73]Institut für Physik, Johannes Gutenberg Universität, Mainz, Germany. [74]Institute of High Energy Physics, Chinese Academy of Sciences, Beijing, China. [75]State Key Laboratory of Magnetic Resonance and Atomic and Molecular Physics, Wuhan Institute of Physics and Mathematics, Chinese Academy of Sciences, Wuhan, China. [76]Department of Physics, University of Cincinnati, Cincinnati, USA.

Endnotes

[a] The ALIA proposal in Europe [111] and the DECIGO proposal in Japan [112] have been aimed at a similar frequency range, and the scientific interest of this frequency range has recently been stressed in [113, 114] and [115].

[b] This projection assumes that the gravity gradient noise (GGN) can be mitigated, as discussed later.

[c] It has been pointed out in [30] that, in addition to the constraints displayed in Fig. 2, there are potential constraints on quadratically-coupled DM from Big Bang Nucleosynthesis, which merit detailed evaluation.

[d] This figure also indicates a typical gravitational gradient noise (GGN) level for a km-scale ground-based detector. In order for such a detector to reach its potential, this GGN would need to be significantly mitigated. Thanks to precise characterization of GGN correlation properties [116], it is possible to reduce GGN using detectors geometries based on arrays of Atom interferometers [93]. A similar GGN level in a km-scale ground-based detector is relevant for the other GW topics discussed below.

[e] In addition to this primary astrophysical programme, we note that AEDGE would also be able to measure GWs from galactic white-dwarf (or other) binaries with orbital periods lass than about a minute, a possibility whose interest has been heightened recently by the observation of a binary with orbital period below 7 minutes [117].

[f] We will benefit from in-team expertise in numerical calculations of BECs—see [118] and references therein.

Publisher's Note

Springer Nature remains neutral with regard to jurisdictional claims in published maps and institutional affiliations.

Received: 23 October 2019 Accepted: 4 February 2020 Published online: 04 March 2020

References

1. CERN. Workshop on atomic experiments for dark matter and gravity exploration. https://indico.cern.ch/event/830432/.
2. Planck collaboration, Aghanim N, et al. Planck 2018 results. VI. Cosmological parameters. arXiv:1807.06209.
3. LIGO Scientific collaboration, Aasi J, et al. Advanced LIGO. Class Quantum Gravity. 2015;32:074001. https://doi.org/10.1088/0264-9381/32/7/074001. arXiv:1411.4547.

4. VIRGO collaboration, Acernese F, et al. Advanced Virgo: a second-generation interferometric gravitational wave detector. Class Quantum Gravity. 2015;32:024001. https://doi.org/10.1088/0264-9381/32/2/024001. arXiv:1408.3978.
5. KAGRA collaboration, Somiya K. Detector configuration of KAGRA: the Japanese cryogenic gravitational-wave detector. Class Quantum Gravity. 2012;29:124007. https://doi.org/10.1088/0264-9381/29/12/124007. arXiv:1111.7185.
6. Unnikrishnan CS. IndIGO and LIGO-India: scope and plans for gravitational wave research and precision metrology in India. Int J Mod Phys D. 2013;22:1341010. https://doi.org/10.1142/S0218271813410101. arXiv:1510.06059.
7. Punturo M, et al. The Einstein telescope: a third-generation gravitational wave observatory. Class Quantum Gravity. 2010;27:194002. https://doi.org/10.1088/0264-9381/27/19/194002.
8. Sathyaprakash B, et al. Scientific objectives of Einstein telescope. Class Quantum Gravity. 2012;29:124013. https://doi.org/10.1088/0264-9381/29/12/124013. arXiv:1206.0331.
9. Reitze D, et al. Cosmic Explorer: the U.S. contribution to gravitational-wave astronomy beyond LIGO. Bull Am Astron Soc. 2019;51:035. arXiv:1907.04833.
10. Guo Z-K, Cai R-G, Zhang Y-Z. Taiji program: gravitational-wave sources. arXiv:1807.09495.
11. Luo J, Chen L-S, Duan H-Z, Gong Y-G, Hu S, Ji J, et al. TianQin: a space-borne gravitational wave detector. Class Quantum Gravity. 2016;33:035010. https://doi.org/10.1088/0264-9381/33/3/035010.
12. Pezzè L, Smerzi A, Oberthaler MK, Schmied R, Treutlein P. Quantum metrology with nonclassical states of atomic ensembles. Rev Mod Phys. 2018;90:035005. https://doi.org/10.1103/RevModPhys.90.035005. arXiv:1609.01609.
13. XENON collaboration, Aprile E, et al. Dark matter search results from a one ton-year exposure of XENON1T. Phys Rev Lett. 2018;121:111302. https://doi.org/10.1103/PhysRevLett.121.111302. arXiv:1805.12562.
14. Battaglieri M, et al. US cosmic visions: new ideas in dark matter 2017: community report. In: U.S. cosmic visions: new ideas in dark matter. College Park, MD, USA. March 23–25, 2017. 2017. http://lss.fnal.gov/archive/2017/conf/fermilab-conf-17-282-ae-ppd-t.pdf. arXiv:1707.04591.
15. Preskill J, Wise MB, Wilczek F. Cosmology of the invisible axion. Phys Lett B. 1983;120:127–32. https://doi.org/10.1016/0370-2693(83)90637-8.
16. Abbott LF, Sikivie P. A cosmological bound on the invisible axion. Phys Lett B. 1983;120:133–6. https://doi.org/10.1016/0370-2693(83)90638-X.
17. Dine M, Fischler W. The not so harmless axion. Phys Lett B. 1983;120:137–41. https://doi.org/10.1016/0370-2693(83)90639-1.
18. Geraci AA, Derevianko A. Sensitivity of atom interferometry to ultralight scalar field dark matter. Phys Rev Lett. 2016;117:261301. https://doi.org/10.1103/PhysRevLett.117.261301. arXiv:1605.04048.
19. Arvanitaki A, Graham PW, Hogan JM, Rajendran S, Van Tilburg K. Search for light scalar dark matter with atomic gravitational wave detectors. Phys Rev D. 2018;97:075020. https://doi.org/10.1103/PhysRevD.97.075020. arXiv:1606.04541.
20. Arvanitaki A, Huang J, Van Tilburg K. Searching for dilaton dark matter with atomic clocks. Phys Rev D. 2015;91:015015. https://doi.org/10.1103/PhysRevD.91.015015. arXiv:1405.2925.
21. Stadnik YV, Flambaum VV. Can dark matter induce cosmological evolution of the fundamental constants of nature? Phys Rev Lett. 2015;115:201301. https://doi.org/10.1103/PhysRevLett.115.201301. arXiv:1503.08540.
22. Damour T, Donoghue JF. Phenomenology of the equivalence principle with light scalars. Class Quantum Gravity. 2010;27:202001. https://doi.org/10.1088/0264-9381/27/20/202001. arXiv:1007.2790.
23. Damour T, Donoghue JF. Equivalence principle violations and couplings of a light dilaton. Phys Rev D. 2010;82:084033. https://doi.org/10.1103/PhysRevD.82.084033. arXiv:1007.2792.
24. Berge J, Brax P, Métris G, Pernot-Borras M, Touboul P, Uzan J-P. MICROSCOPE mission: first constraints on the violation of the weak equivalence principle by a light scalar dilaton. Phys Rev Lett. 2018;120:141101. https://doi.org/10.1103/PhysRevLett.120.141101. arXiv:1712.00483.
25. Hees A, Minazzoli O, Savalle E, Stadnik YV, Wolf P. Violation of the equivalence principle from light scalar dark matter. Phys Rev D. 2018;98:064051. https://doi.org/10.1103/PhysRevD.98.064051. arXiv:1807.04512.
26. Schlamminger S, Choi KY, Wagner TA, Gundlach JH, Adelberger EG. Test of the equivalence principle using a rotating torsion balance. Phys Rev Lett. 2008;100:041101. https://doi.org/10.1103/PhysRevLett.100.041101. arXiv:0712.0607.
27. Wagner TA, Schlamminger S, Gundlach JH, Adelberger EG. Torsion-balance tests of the weak equivalence principle. Class Quantum Gravity. 2012;29:184002. https://doi.org/10.1088/0264-9381/29/18/184002. arXiv:1207.2442.
28. Van Tilburg K, Leefer N, Bougas L, Budker D. Search for ultralight scalar dark matter with atomic spectroscopy. Phys Rev Lett. 2015;115:011802. https://doi.org/10.1103/PhysRevLett.115.011802. arXiv:1503.06886.
29. Hees A, Guena J, Abgrall M, Bize S, Wolf P. Searching for an oscillating massive scalar field as a dark matter candidate using atomic hyperfine frequency comparisons. Phys Rev Lett. 2016;117:061301. https://doi.org/10.1103/PhysRevLett.117.061301. arXiv:1604.08514.
30. Stadnik YV, Flambaum VV. Searching for dark matter and variation of fundamental constants with laser and maser interferometry. Phys Rev Lett. 2015;114:161301. https://doi.org/10.1103/PhysRevLett.114.161301. arXiv:1412.7801.
31. Graham PW, Kaplan DE, Mardon J, Rajendran S, Terrano WA, Trahms L, et al. Spin precession experiments for light axionic dark matter. Phys Rev D. 2018;97:055006. https://doi.org/10.1103/PhysRevD.97.055006. arXiv:1709.07852.
32. Graham PW, Kaplan DE, Mardon J, Rajendran S, Terrano WA. Dark matter direct detection with accelerometers. Phys Rev D. 2016;93:075029. https://doi.org/10.1103/PhysRevD.93.075029. arXiv:1512.06165.
33. O'Hare CAJ, McCabe C, Evans NW, Myeong G, Belokurov V. Dark matter hurricane: measuring the S1 stream with dark matter detectors. Phys Rev D. 2018;98:103006. https://doi.org/10.1103/PhysRevD.98.103006. arXiv:1807.09004.
34. Roberts BM, Derevianko A. Precision measurement noise asymmetry and its annual modulation as a dark matter signature. arXiv:1803.00617.
35. LIGO Scientific, Virgo collaboration, Abbott BP, et al. GWTC-1: a gravitational-wave transient catalog of compact binary mergers observed by LIGO and Virgo during the first and second observing runs. Phys Rev X. 2019;9:031040. https://doi.org/10.1103/PhysRevX.9.031040. arXiv:1811.12907.
36. LISA collaboration Audley H, et al. Laser interferometer space antenna. arXiv:1702.00786.
37. van Haasteren R, et al. Placing limits on the stochastic gravitational-wave background using European Pulsar Timing Array data. Mon Not R Astron Soc. 2011;414:3117–28. https://doi.org/10.1111/j.1365-2966.2011.18613.x. arXiv:1103.0576.

38. Canuel B, et al. Exploring gravity with the MIGA large scale atom interferometer. Sci Rep. 2018;8:14064. https://doi.org/10.1038/s41598-018-32165-z. arXiv:1703.02490.
39. Zhan M-S, et al. ZAIGA: Zhaoshan Long-baseline Atom Interferometer Gravitation Antenna. Int J Mod Phys D. 2019;28:1940005. https://doi.org/10.1142/S0218271819400054. arXiv:1903.09288.
40. MAGIS collaboration, Graham PW, Hogan JM, Kasevich MA, Rajendran S, Romani RW. Mid-band gravitational wave detection with precision atomic sensors. arXiv:1711.02225.
41. Bouyer P. MIGA and ELGAR: new perspectives for low frequency gravitational wave observation using atom interferometry. 2018. https://indico.obspm.fr/event/58/contributions/214/attachments/88/98/Slides-bouyer2018_06_21_MIGA_GDR.pdf.
42. AION Core Team collaboration, Bongs K, et al. An Atom Interferometer Observatory and Network (AION) for the exploration of ultra-light dark matter and mid-frequency gravitational waves. 2019. https://www.hep.ph.ic.ac.uk/AION-Project/.
43. Magorrian J, et al. The demography of massive dark objects in galaxy centers. Astron J. 1998;115:2285. https://doi.org/10.1086/300353. arXiv:astro-ph/9708072.
44. Kauffmann G, Haehnelt M. A unified model for the evolution of galaxies and quasars. Mon Not R Astron Soc. 2000;311:576–88. https://doi.org/10.1046/j.1365-8711.2000.03077.x. arXiv:astro-ph/9906493.
45. Event Horizon Telescope collaboration Akiyama K, et al. First M87 event horizon telescope results. I. The shadow of the supermassive black hole. Astrophys J. 2019;875:L1. https://doi.org/10.3847/2041-8213/ab0ec7.
46. Rees MJ. Black hole models for active galactic nuclei. Annu Rev Astron Astrophys. 1984;22:471–506. https://doi.org/10.1146/annurev.aa.22.090184.002351.
47. Mezcua M. Observational evidence for intermediate-mass black holes. Int J Mod Phys D. 2017;26:1730021. https://doi.org/10.1142/S021827181730021X. arXiv:1705.09667.
48. Katz H, Sijacki D, Haehnelt MG. Seeding high redshift QSOs by collisional runaway in primordial star clusters. Mon Not R Astron Soc. 2015;451:2352. https://doi.org/10.1093/mnras/stv1048.
49. Volonteri M, Haardt F, Madau P. The assembly and merging history of supermassive black holes in hierarchical models of galaxy formation. Astrophys J. 2003;582:559–73. https://doi.org/10.1086/344675. arXiv:astro-ph/0207276.
50. Volonteri M, Lodato G, Natarajan P. The evolution of massive black hole seeds. Mon Not R Astron Soc. 2008;383:1079. https://doi.org/10.1111/j.1365-2966.2007.12589.x. arXiv:0709.0529.
51. Erickcek AL, Kamionkowski M, Benson AJ. Supermassive black hole merger rates: uncertainties from halo merger theory. Mon Not R Astron Soc. 2006;371:1992–2000. https://doi.org/10.1111/j.1365-2966.2006.10838.x. arXiv:astro-ph/0604281.
52. Heger A, Fryer CL, Woosley SE, Langer N, Hartmann DH. How massive single stars end their life. Astrophys J. 2003;591:288–300. https://doi.org/10.1086/375341. arXiv:astro-ph/0212469.
53. Sesana A. Prospects for multiband gravitational-wave astronomy after GW150914. Phys Rev Lett. 2016;116:231102. https://doi.org/10.1103/PhysRevLett.116.231102. arXiv:1602.06951.
54. Graham PW, Jung S. Localizing gravitational wave sources with single-baseline atom interferometers. Phys Rev D. 2018;97:024052. https://doi.org/10.1103/PhysRevD.97.024052. arXiv:1710.03269.
55. Carson Z, Yagi K. Multi-band gravitational wave tests of general relativity. Class Quantum Gravity. 2020;37(2):02LT01. https://doi.org/10.1088/1361-6382/ab5c9a. arXiv:1905.13155.
56. Bern Z, Cheung C, Roiban R, Shen C-H, Solon MP, Zeng M. Scattering amplitudes and the conservative Hamiltonian for binary systems at third post-minkowskian order. Phys Rev Lett. 2019;122:201603. https://doi.org/10.1103/PhysRevLett.122.201603. arXiv:1901.04424.
57. Ellis J, Fairbairn M, Lewicki M, Vaskonen V, Wickens A. Intergalactic magnetic fields from first-order phase transitions. J Cosmol Astropart Phys. 2019;1909:019. https://doi.org/10.1088/1475-7516/2019/09/019. arXiv:1907.04315.
58. Ellis J, Lewicki M, No JM. On the maximal strength of a first-order electroweak phase transition and its gravitational wave signal. J Cosmol Astropart Phys. 2019;1904:003. https://doi.org/10.1088/1475-7516/2019/04/003. arXiv:1809.08242.
59. Ellis J, Lewicki M, No JM, Vaskonen V. Gravitational wave energy budget in strongly supercooled phase transitions. J Cosmol Astropart Phys. 2019;1906:024. https://doi.org/10.1088/1475-7516/2019/06/024. arXiv:1903.09642.
60. FCC collaboration Abada A, et al. FCC physics opportunities. Eur Phys J C. 2019;79:474. https://doi.org/10.1140/epjc/s10052-019-6904-3.
61. SKA collaboration, Bacon DJ, et al. Cosmology with phase 1 of the square kilometre array: Red Book 2018: technical specifications and performance forecasts. Publ Astron Soc Aust. Submitted 2018. arXiv:1811.02743.
62. Cui Y, Lewicki M, Morrissey DE, Wells JD. Probing the pre-BBN universe with gravitational waves from cosmic strings. J High Energy Phys. 2019;01:081. https://doi.org/10.1007/JHEP01(2019)081. arXiv:1808.08968.
63. Tino GM, et al. SAGE: a proposal for a Space Atomic Gravity Explorer. Eur Phys J D. 2019;73:228. Topical Issue on Quantum Technologies for Gravitational Physics. arXiv:1907.03867.
64. Becker JK. High-energy neutrinos in the context of multimessenger physics. Phys Rep. 2008;458:173–246. https://doi.org/10.1016/j.physrep.2007.10.006. arXiv:0710.1557.
65. Alonso R, Blas D, Wolf P. Exploring the ultra-light to sub-MeV dark matter window with atomic clocks and co-magnetometers. J High Energy Phys. 2019;07:069. https://doi.org/10.1007/JHEP07(2019)069. arXiv:1810.00889.
66. Peters A, Chung KY, Chu S. High-precision gravity measurements using atom interferometry. Metrologia. 2001;38:25–61. https://doi.org/10.1088/0026-1394/38/1/4.
67. Safronova MS, Budker D, DeMille D, Kimball DFJ, Derevianko A, Clark CW. Search for new physics with atoms and molecules. Rev Mod Phys. 2018;90:025008. https://doi.org/10.1103/RevModPhys.90.025008. arXiv:1710.01833.
68. Dimopoulos S, Graham PW, Hogan JM, Kasevich MA. General relativistic effects in atom interferometry. Phys Rev D. 2008;78:042003. https://doi.org/10.1103/PhysRevD.78.042003. arXiv:0802.4098.
69. Uzan J-P. The fundamental constants and their variation: observational status and theoretical motivations. Rev Mod Phys. 2003;75:403. https://doi.org/10.1103/RevModPhys.75.403. arXiv:hep-ph/0205340.
70. Martins CJAP, Miñana MV. Consistency of local and astrophysical tests of the stability of fundamental constants. Phys Dark Universe. 2019;25:100301. https://doi.org/10.1016/j.dark.2019.100301. arXiv:1904.07896.
71. Jaffe M, Haslinger P, Xu V, Hamilton P, Upadhye A, Elder B, et al. Testing sub-gravitational forces on atoms from a miniature, in-vacuum source mass. Nat Phys. 2017;13:938. https://doi.org/10.1038/nphys4189. arXiv:1612.05171.

72. Sabulsky DO, Dutta I, Hinds EA, Elder B, Burrage C, Copeland EJ. Experiment to detect dark energy forces using atom interferometry. Phys Rev Lett. 2019;123:061102. https://doi.org/10.1103/PhysRevLett.123.061102. arXiv:1812.08244.
73. Ellis JR, Hagelin JS, Nanopoulos DV, Srednicki M. Search for violations of quantum mechanics. Nucl Phys B. 1984;241:381. https://doi.org/10.1016/0550-3213(84)90053-1.
74. Banks T, Susskind L, Peskin ME. Difficulties for the evolution of pure states into mixed states. Nucl Phys B. 1984;244:125–34. https://doi.org/10.1016/0550-3213(84)90184-6.
75. Ghirardi GC, Rimini A, Weber T. Unified dynamics for microscopic and macroscopic systems. Phys Rev D. 1986;34:470. https://doi.org/10.1103/PhysRevD.34.470.
76. Weinberg S. Lindblad decoherence in atomic clocks. Phys Rev A. 2016;94:042117. https://doi.org/10.1103/PhysRevA.94.042117. arXiv:1610.02537.
77. Chung K-Y, Chiow S-W, Herrmann S, Chu S, Muller H. Atom interferometry tests of local Lorentz invariance in gravity and electrodynamics. Phys Rev D. 2009;80:016002. https://doi.org/10.1103/PhysRevD.80.016002. arXiv:0905.1929.
78. Graham PW, Hogan JM, Kasevich MA, Rajendran S. A new method for gravitational wave detection with atomic sensors. Phys Rev Lett. 2013;110:171102. https://doi.org/10.1103/PhysRevLett.110.171102. arXiv:1206.0818.
79. Graham PW, Hogan JM, Kasevich MA, Rajendran S. Resonant mode for gravitational wave detectors based on atom interferometry. Phys Rev D. 2016;94:104022. https://doi.org/10.1103/PhysRevD.94.104022. arXiv:1606.01860.
80. Hu L, Poli N, Salvi L, Tino GM. Atom interferometry with the Sr optical clock transition. Phys Rev Lett. 2017;119:263601. https://doi.org/10.1103/PhysRevLett.119.263601.
81. Snadden MJ, McGuirk JM, Bouyer P, Haritos KG, Kasevich MA. Measurement of the Earth's gravity gradient with an atom interferometer-based gravity gradiometer. Phys Rev Lett. 1998;81:971–4. https://doi.org/10.1103/PhysRevLett.81.971.
82. Sorrentino F, Bodart Q, Cacciapuoti L, Lien YH, Prevedelli M, Rosi G, et al. Sensitivity limits of a Raman atom interferometer as a gravity gradiometer. Phys Rev A. 2014;89:023607. https://doi.org/10.1103/PhysRevA.89.023607. arXiv:1312.3741.
83. Hogan JM, Kasevich MA. Atom interferometric gravitational wave detection using heterodyne laser links. Phys Rev A. 2016;94:033632. https://doi.org/10.1103/PhysRevA.94.033632. arXiv:1501.06797.
84. Rudolph J, Wilkason T, Nantel M, Swan H, Holland CM, Jiang Y, et al. Large momentum transfer clock atom interferometry on the 689 nm intercombination line of strontium. arXiv:1910.05459.
85. Dimopoulos S, Graham PW, Hogan JM, Kasevich MA, Rajendran S. An Atomic Gravitational Wave Interferometric Sensor (AGIS). Phys Rev D. 2008;78:122002. https://doi.org/10.1103/PhysRevD.78.122002. arXiv:0806.2125.
86. Thrane E, Romano JD. Sensitivity curves for searches for gravitational-wave backgrounds. Phys Rev D. 2013;88:124032. https://doi.org/10.1103/PhysRevD.88.124032. arXiv:1310.5300.
87. Liu L, Lü D-S, Chen W-B, Li T, Qu Q-Z, Wang B, et al. In-orbit operation of an atomic clock based on laser-cooled 87Rb atoms. Nat Commun. 2018;9:2760. https://doi.org/10.1038/s41467-018-05219-z.
88. Becker D, et al. Space-borne Bose–Einstein condensation for precision interferometry. Nature. 2018;562:391. https://doi.org/10.1038/s41586-018-0605-1.
89. Elliott ER, Krutzik MC, Williams JR, Thompson RJ, Aveline DC. NASA's Cold Atom Lab (CAL): system development and ground test status. npj Microgravity. 2018;4:16. https://doi.org/10.1038/s41526-018-0049-9.
90. Lezius M, et al. Space-borne frequency comb metrology. Optica. 2016;3:1381. https://doi.org/10.1364/OPTICA.3.001381.
91. Dinkelaker A, et al. Autonomous frequency stabilization of two extended-cavity diode lasers at the potassium wavelength on a sounding rocket. Appl Opt. 2017;56:1388. https://doi.org/10.1364/AO.56.001388.
92. Döringshoff K, et al. Iodine frequency reference on a sounding rocket. Phys Rev Appl. 2019;11:054068. https://doi.org/10.1103/PhysRevApplied.11.054068.
93. Chaibi W, Geiger R, Canuel B, Bertoldi A, Landragin A, Bouyer P. Low frequency gravitational wave detection with ground based atom interferometer arrays. Phys Rev D. 2016;93:021101. https://doi.org/10.1103/PhysRevD.93.021101. arXiv:1601.00417.
94. Rosi G, Sorrentino F, Cacciapuoti L, Prevedelli M, Tino GM. Precision measurement of the Newtonian gravitational constant using cold atoms. Nature. 2014;510:518. https://doi.org/10.1038/nature13433. arXiv:1412.7954.
95. Tino GM, et al. Ultracold atoms and precision measurements. http://coldatoms.lens.unifi.it.
96. ELGAR collaboration, Sabulsky D. The European Laboratory for Gravitation and Atom-interferometric Research (ELGAR) Project. 2019. https://indico.cern.ch/event/830432/contributions/3497166/attachments/1883894/3104651/sabulsky_ELGAR_CERN_2019.pdf.
97. Cacciapuoti L, Salomon C. Space clocks and fundamental tests: the ACES experiment. Eur Phys J Spec Top. 2009;172:57. https://doi.org/10.1140/epjst/e2009-01041-7.
98. Laurent P, Massonnet D, Cacciapuoti L, Salomon C. The ACES/PHARAO space mission. C R Phys. 2015;16(5):540. https://doi.org/10.1016/j.crhy.2015.05.002.
99. Müntinga H, et al. Interferometry with Bose-Einstein condensates in microgravity. Phys Rev Lett. 2013;110:093602. https://doi.org/10.1103/PhysRevLett.110.093602. arXiv:1301.5883.
100. BECCAL collaboration, Becker D, et al. BECCAL science overview. 2019. https://custom.cvent.com/216E523D934443CA9F514B796474A210/files/f7a0cce2d06f4e2182eaec7af912d5bf.pdf.
101. Barrett B, Antoni-Micollier L, Chichet L, Battelier B, Lévèque T, Landragin A, et al. Dual matter-wave inertial sensors in weightlessness. Nat Commun. 2016;7:13786. https://doi.org/10.1038/ncomms13786.
102. Condon G, et al. All-optical Bose–Einstein condensates in microgravity. Phys Rev Lett. 2019;123:240402. https://doi.org/10.1103/PhysRevLett.123.240402. arXiv:1906.10063.
103. Bongs K, et al. Development of a strontium optical lattice clock for the SOC mission on the ISS. C R Phys. 2015;16(5):553. https://doi.org/10.1016/j.crhy.2015.03.009.
104. Origlia S, et al. Towards an optical clock for space: compact, high-performance optical lattice clock based on bosonic atoms. Phys Rev A. 2018;98:053443. https://doi.org/10.1103/PhysRevA.98.053443.
105. Aguilera D, et al. STE-QUEST—test of the universality of free fall using cold atom interferometry. Class Quantum Gravity. 2014;31:115010. https://doi.org/10.1088/0264-9381/31/11/115010. arXiv:1312.5980.
106. Lacour S, et al. SAGE: finding IMBH in the black hole desert. Class Quantum Gravity. 2019;36:195005. https://doi.org/10.1088/1361-6382/ab3583. arXiv:1811.04743.

107. Gao D, Wang J, Zhan M. Atomic Interferometric Gravitational-Wave Space Observatory (AIGSO). Commun Theor Phys. 2018;69:37. https://doi.org/10.1088/0253-6102/69/1/37.
108. Wolf P, et al. Quantum physics exploring gravity in the outer solar system: the SAGAS project. Exp Astron. 2009;23(2):651. https://doi.org/10.1007/s10686-008-9118-5.
109. Tino GM, et al. Atom interferometers and optical atomic clocks: new quantum sensors for fundamental physics experiments in space. Nucl Phys B, Proc Suppl. 2007;166:159. https://doi.org/10.1016/j.nuclphysbps.2006.12.061.
110. Sorrentino F, et al. A compact atom interferometer for future space missions. Microgravity Sci Technol. 2010;22:551. https://doi.org/10.1007/s12217-010-9240-7.
111. Bender PL, Begelman MC, Gair JR. Possible LISA follow-on mission scientific objectives. Class Quantum Gravity. 2013;30:165017. https://doi.org/10.1088/0264-9381/30/16/165017.
112. Kawamura S, et al. The Japanese space gravitational wave antenna: DECIGO. Class Quantum Gravity. 2011;28:094011. https://doi.org/10.1088/0264-9381/28/9/094011.
113. Mandel I, Sesana A, Vecchio A. The astrophysical science case for a decihertz gravitational-wave detector. Class Quantum Gravity. 2018;35:054004. https://doi.org/10.1088/1361-6382/aaa7e0. arXiv:1710.11187.
114. Baker J, et al. Space based gravitational wave astronomy beyond LISA (Astro2020 APC white paper). arXiv:1907.11305.
115. Kuns KA, Yu H, Chen Y, Adhikari RX. Astrophysics and cosmology with a deci-hertz gravitational-wave detector: TianGO. arXiv:1908.06004.
116. Junca J, et al. Characterizing Earth gravity field fluctuations with the MIGA antenna for future Gravitational Wave detectors. Phys Rev D. 2019;99:104026. https://doi.org/10.1103/PhysRevD.99.104026. arXiv:1902.05337.
117. Burdge KB, et al. General relativistic orbital decay in a seven-minute-orbital-period eclipsing binary system. Nature. 2019;571:528–31. https://doi.org/10.1038/s41586-019-1403-0. arXiv:1907.11291.
118. Kishor Kumar R, et al. C and Fortran OpenMP programs for rotating Bose–Einstein condensates. Comput Phys Commun. 2019;240:74. https://doi.org/10.1016/j.cpc.2019.03.004. arXiv:1906.06327.

Submit your manuscript to a SpringerOpen journal and benefit from:

- ► Convenient online submission
- ► Rigorous peer review
- ► Open access: articles freely available online
- ► High visibility within the field
- ► Retaining the copyright to your article

Submit your next manuscript at ► springeropen.com